Overview of Nucleon Form Factor Measurements

Prof. Andrew Puckett

University of Connecticut

QNP2022 – The 9th International Conference on Quarks and Nuclear Physics

Sept. 6, 2022

UCONN

Electron-Nucleon Scattering in QED

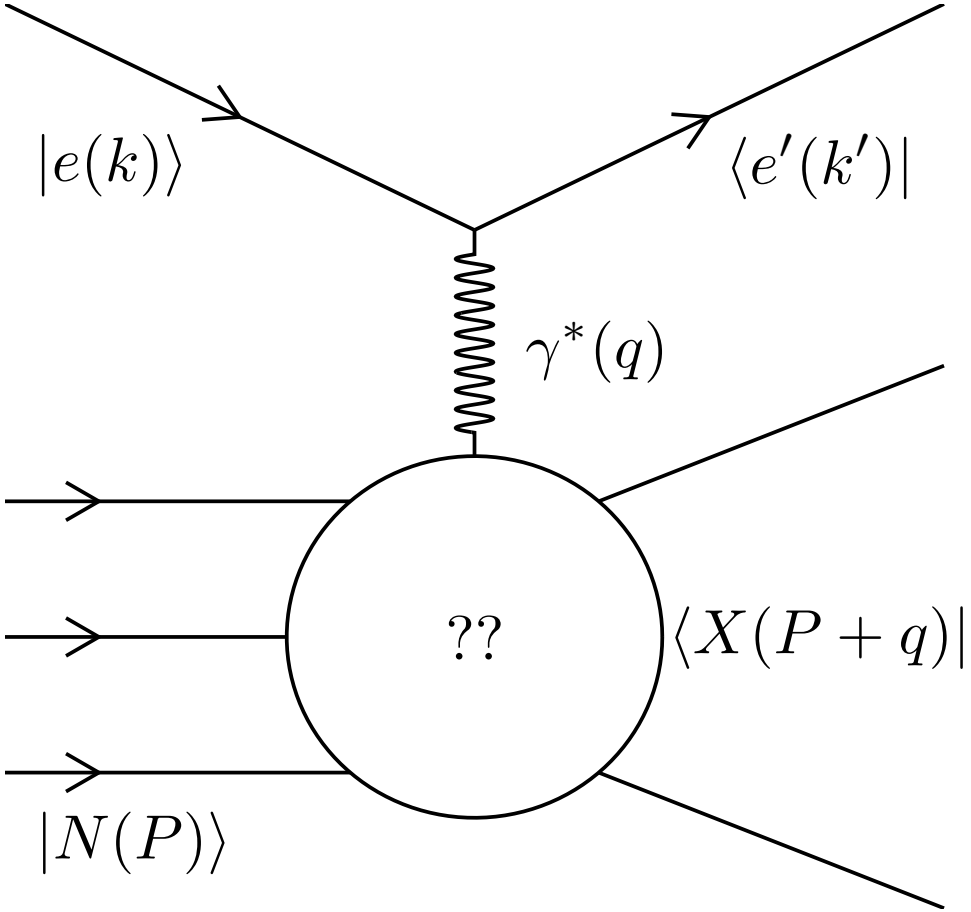

$$Q^2 \equiv -q^2 = -(k-k')^2$$

Feynman diagram for electron-nucleon scattering in the one-photon-exchange (Born) approximation

$$\alpha \equiv \frac{e^2}{4\pi\epsilon_0\hbar c} = \frac{1}{137.035\ 999\ 084(21)} \quad \text{(PDG 2019)}$$

- Charged leptons (e.g., electrons) interact with the charged constituents of nucleons and nuclei predominantly via electromagnetic (EM) interaction (but also weak interaction).
- Electrons are point-like
- EM interaction is "weak"→low-order QED perturbation theory works well→"clean" theoretical interpretation
- EM interaction is well-described by the exchange of a single virtual photon of four-momentum q.
- Analogous to impulse approximation in classical mechanics
- Availability of high-quality electron beams w/ well-defined properties (energy, intensity, polarization, etc.) makes electron scattering a precision probe of nuclear structure

Electron Scattering from a static charge distribution in QED

$$\frac{d\sigma}{d\Omega} = \left(\frac{d\sigma}{d\Omega}\right)_{Mott} |F(\mathbf{q})|^2$$

$$\left(\frac{d\sigma}{d\Omega}\right)_{Mott} \equiv \frac{\alpha^2(\hbar c)^2}{4E_e^2 \sin^4\frac{\theta}{2}} \frac{E_e'}{E_e} \cos^2\frac{\theta}{2}$$

$$F(\mathbf{q}) = \int \rho(\mathbf{x}) e^{i\mathbf{q}\cdot\mathbf{x}} d^3x$$

- $\left(\frac{d\sigma}{d\Omega}\right)_{Mott}$ describes the scattering of ultra-relativistic, spin-1/2 electrons from a point-like, spin-less target of charge *e*. Very similar to the familiar Rutherford cross section describing pure Coulomb scattering in classical mechanics (or non-relativistic quantum mechanics)
- Electron scattering cross section factorizes as the product of σ_{Mott} and the square of the *form factor* $F(\vec{\boldsymbol{q}})$, which is the three-dimensional Fourier transform of the charge density with respect to the three-momentum transfer $\boldsymbol{q} = \boldsymbol{k} - \boldsymbol{k}'$

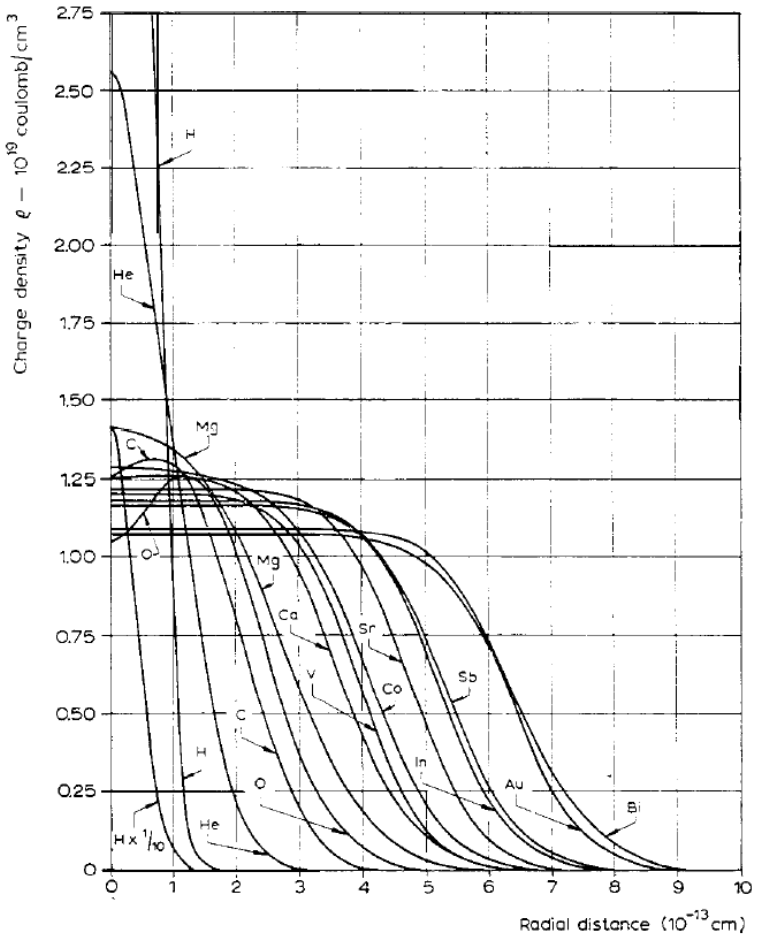

Nuclear Charge Densities from electron scattering (R. Hofstadter Nobel Prize Lecture)

Elastic Electron-Nucleon Scattering and Form Factors

- The Dirac (F_1) and Paul (F_2) form factors describe the most general form of the virtual photon-nucleon vertex function consistent with the symmetries of QED; namely, Lorentz invariance, parity conservation and gauge invariance/current conservation
- They are real-valued functions of the (space-like) squared four-momentum transfer $q^2 = (k - k')^2 < 0$.
- Experimental observables sensitive to form factors include differential cross sections and double-spin asymmetries involving polarized e^- beams and/or targets

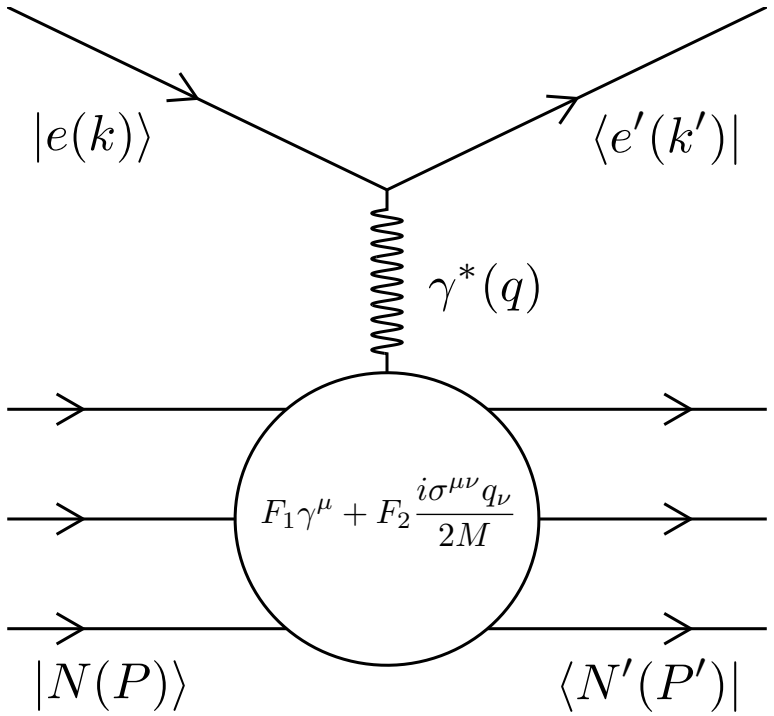

Feynman Diagram for elastic $eN \to eN$ scattering in OPE approximation

$$\text{Invariant amplitude: } \mathcal{M} = 4\pi\alpha\bar{u}(k')\gamma^\mu u(k)\left(\frac{g_{\mu\nu}}{q^2}\right)\bar{u}(P')\Gamma^\nu u(P)$$

$$\gamma^* N \text{ vertex function: } \Gamma^\mu = F_1(q^2)\gamma^\mu + \frac{i\sigma^{\mu\nu}q_\nu}{2M}F_2(q^2)$$

$$\text{Sachs FF: } G_E = F_1 - \tau F_2$$

$$G_M = F_1 + F_2$$

$$\text{Rosenbluth Formula: } \frac{d\sigma}{d\Omega_e} = \left(\frac{d\sigma}{d\Omega_e}\right)_{\text{Mott}} \frac{\epsilon G_E^2 + \tau G_M^2}{\epsilon(1+\tau)}$$

$$\tau \equiv \frac{Q^2}{4M^2}$$

$$\epsilon \equiv \left[1 + 2(1+\tau)\tan^2\left(\frac{\theta_e}{2}\right)\right]^{-1}$$

The Nobel Prize in Physics, 1961 (R. Hofstadter)

"for his pioneering studies of electron scattering in atomic nuclei and for his thereby achieved discoveries concerning the structure of the nucleons"

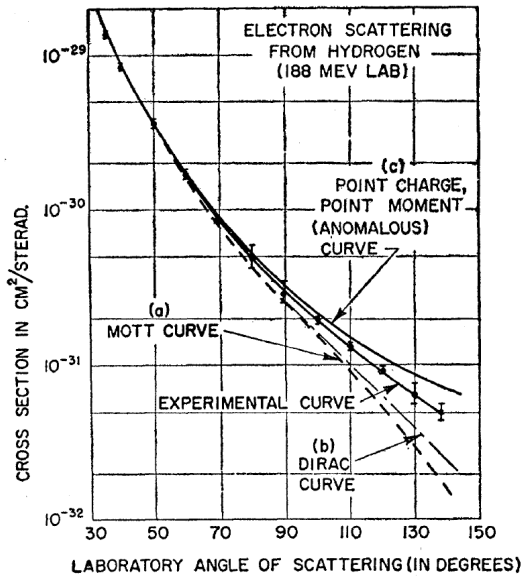

FIG. 24. Electron scattering from the proton at an incident energy of 188 Mev. The experimental points lie below the point-charge point-moment curve of Rosenbluth, indicating finite size effects.

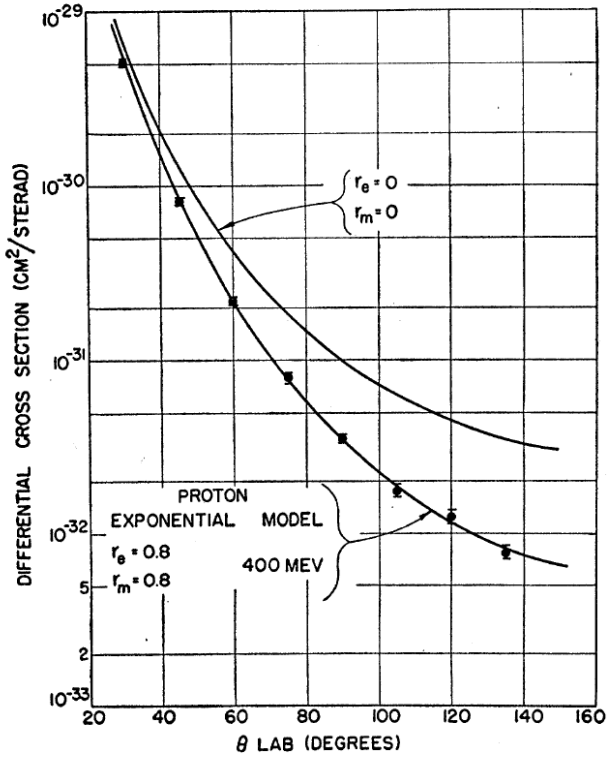

FIG. 26. Typical angular distribution for elastic scattering of 400-Mev electrons against protons. The solid line is a theoretical curve for a proton of finite extent. The model providing the theoretical curve is an exponential with rms radii $=0.80\times10^{-13}$ cm.

Figures from [Rev. Mod. Phys, 28, 214 (1956)]

Rosenbluth Separations of the Proton FFs: Examples

Rosenbluth Formula: $$\frac{d\sigma}{d\Omega_e} = \left(\frac{d\sigma}{d\Omega_e}\right)_{\text{Mott}} \frac{\epsilon G_E^2 + \tau G_M^2}{\epsilon(1+\tau)}$$

Reduced Cross Section: $$\sigma_R \equiv \epsilon(1+\tau)\frac{\sigma_{\text{Measured}}}{\sigma_{\text{Mott}}} \overset{\text{OPE}}{=} \epsilon G_E^2 + \tau G_M^2$$

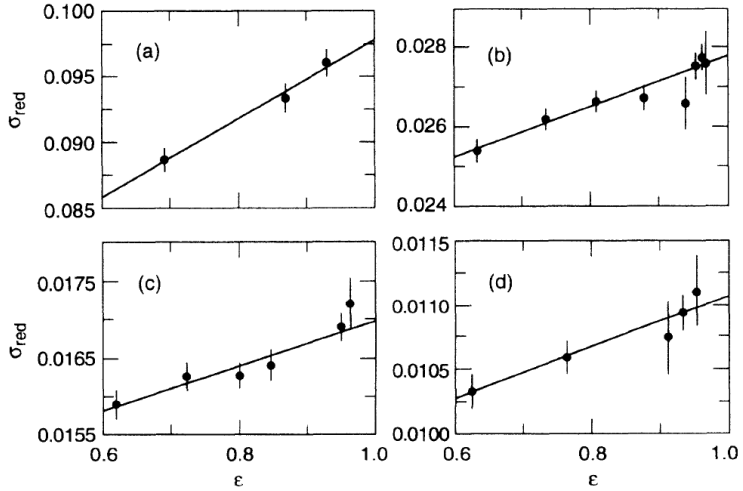

FIG. 7. The linear Rosenbluth fits used for extracting the elastic form factors at (a) $Q^2 = 1.0$, (b) $Q^2 = 2.0$, (c) $Q^2 = 2.5$, and (d) $Q^2 = 3.0$ (GeV/c)^2. Error bars indicate combined (statistical plus point-to-point systematic) uncertainties. Cross section normalization uncertainties of ±1.9% are not shown.

Walker *et al.,* Phys. Rev. D 49, 5671 (1994)

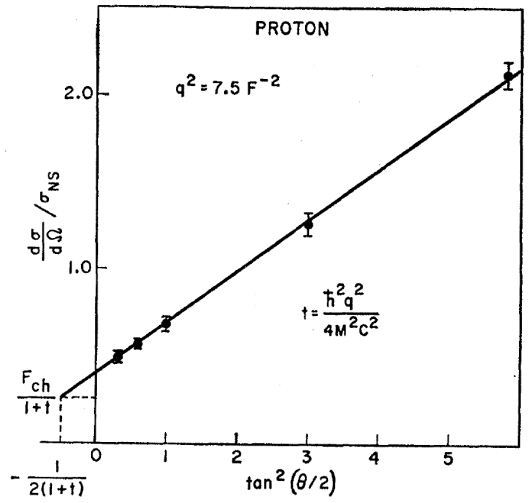

(a)

Janssens *et al.,* Phys. Rev. 142, 922 (1966)

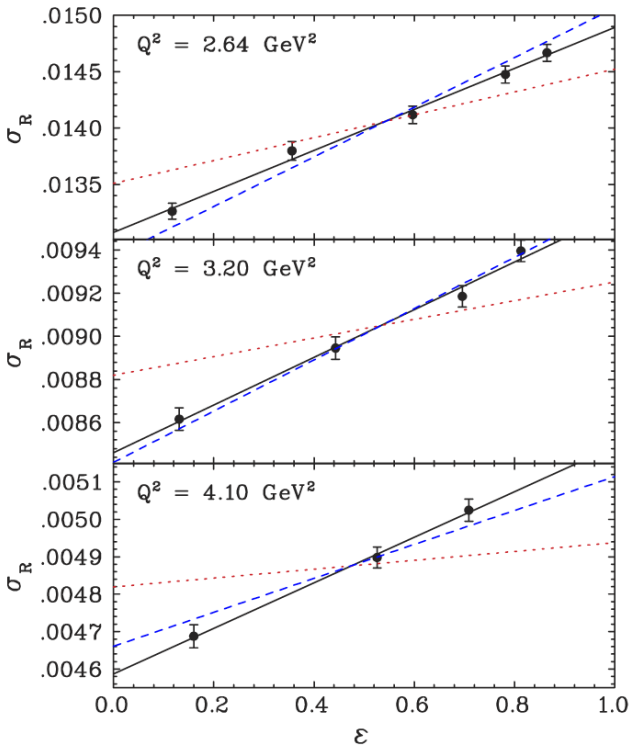

FIG. 2 (color online). Reduced cross sections as a function of ε. The solid line is a linear fit to the reduced cross sections, the dashed line shows the slope expected from scaling ($\mu_p G_E/G_M = 1$), and the dotted line shows the slope predicted by the polarization transfer experiments [6].

Qattan *et al.,* Phys. Rev. Lett. 94, 142301 (2005)

The Proton FFs, ca. 1994

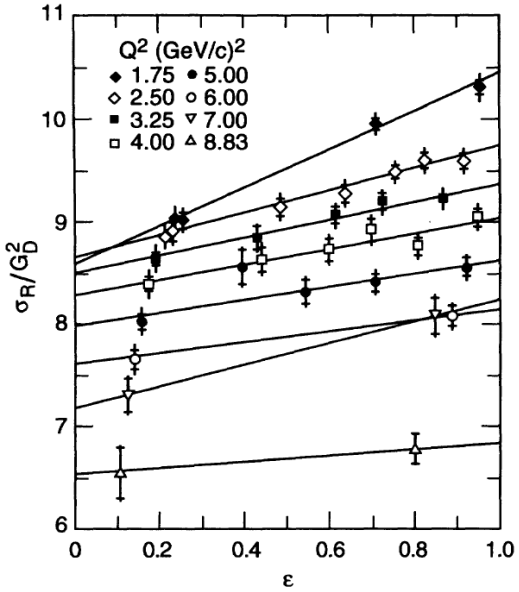

FIG. 22. Reduced cross sections divided by the square of the dipole fit plotted versus ϵ for each value of Q^2. The 1.6 GeV data points correspond to the leftmost point on each line, and the E136 data point is the rightmost point on the $Q^2 = 8.83$ $(\mathrm{GeV}/c)^2$ line. The inner error bars show the statistical error, while the outer error bars show the total point-to-point uncertainty, given by the quadrature sum of the statistical and point-to-point systematic errors. An overall normalization uncertainty of ±1.77% has not been included.

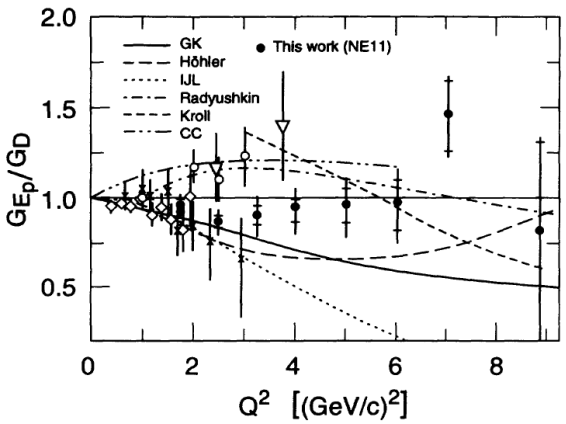

FIG. 23. Extracted values for G_{E_p}/G_D compared with previous data and several models and predictions. The crosses are from Bartel *et al.* Ref. [3], the diamonds from Berger *et al.* Ref. [4], the inverted triangles from Litt *et al.* Ref. [5], and the open circles from Walker *et al.* Ref. [6]. The solid line (GK) is from Ref. [35], the long dashed line (Höhler) is from Ref. [31], the dotted line (IJL) is from Ref. [32], the dashed-dot line (Radyushkin) is from Ref. [37], the short dashed line (Kroll) is from Ref. [40], and the dashed double-dot line (CC) is from Ref. [38].

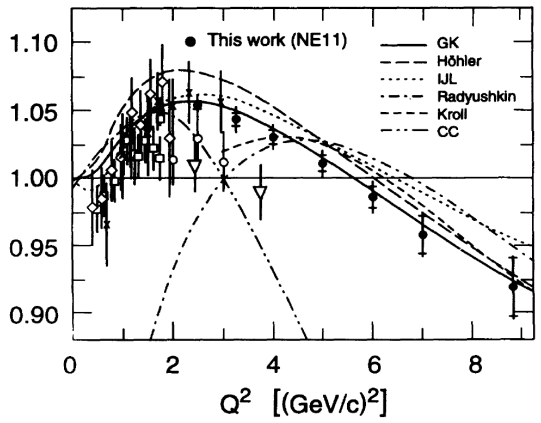

FIG. 24. Extracted values for $G_{M_p}/\mu_p G_D$. The squares are from Bosted *et al.* Ref. [7], otherwise all previous data and model curves are as noted in Fig. 23.

Figures from Andivahis *et al.*, Phys. Rev. D 50, 5491 (1994)

- Most proton electric and magnetic FF Rosenbluth extractions prior to ~2000 can be described to within ~10-20% over the entire measured Q^2 range by the so-called "dipole" form factor:

$$G_E^p \approx G_M^p/\mu_p \approx G_D \equiv \left(1 + \frac{Q^2}{\Lambda^2}\right)^{-2}$$

$$\Lambda^2 = 0.71\ (\mathrm{GeV}/c)^2$$

Polarization Observables in Elastic $eN \to eN$ Scattering

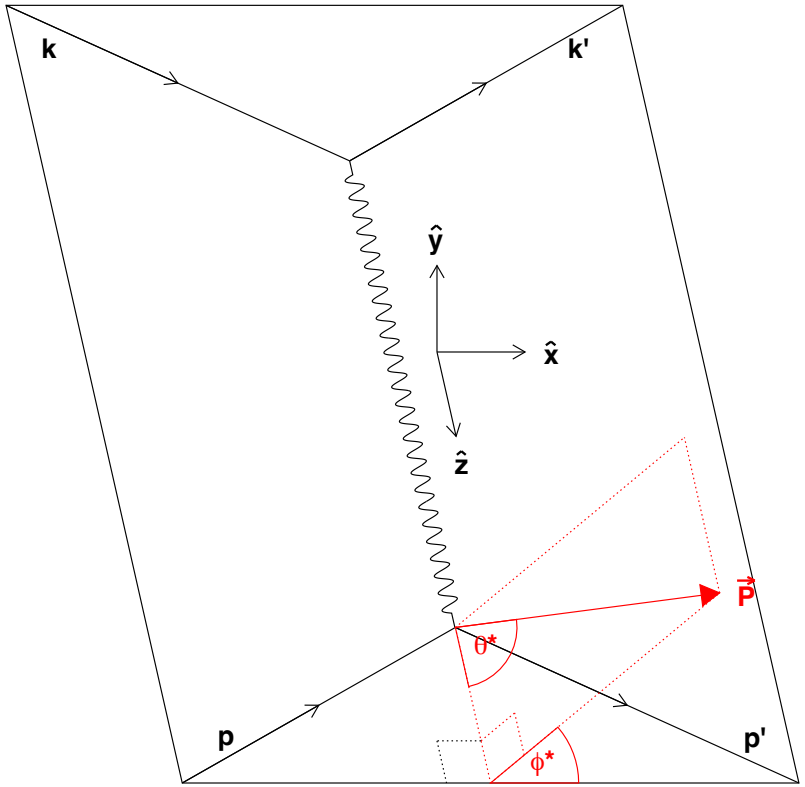

Standard coordinate system and angle definitions for nucleon polarization components in $eN \to eN$

$$A_{eN} \equiv \frac{\sigma_+ - \sigma_-}{\sigma_+ + \sigma_-} = P_{\text{beam}} P_{\text{targ}} \left[A_t \sin\theta^* \cos\phi^* + A_\ell \cos\theta^* \right]$$

$$A_t = -\sqrt{\frac{2\epsilon(1-\epsilon)}{\tau}} \frac{r}{1 + \frac{\epsilon}{\tau} r^2}$$

$$A_\ell = -\frac{\sqrt{1-\epsilon^2}}{1 + \frac{\epsilon}{\tau} r^2}$$

$$r \equiv \frac{G_E}{G_M}$$

$$P_t = P_{beam} A_t$$

$$P_\ell = P_{beam} A_\ell$$

$$\frac{G_E}{G_M} = -\frac{P_t}{P_\ell} \sqrt{\frac{\tau(1+\epsilon)}{2\epsilon}} = -\frac{P_t}{P_\ell} \frac{E_e + E'_e}{2M} \tan\left(\frac{\theta_e}{2}\right)$$

- Polarized beam-polarized target double-spin asymmetry or polarization transfer observables in OPE are sensitive to the electric/magnetic form factor *ratio*, giving enhanced sensitivity to $G_E(G_M)$ for large (small) values of Q^2, as compared to the Rosenbluth method

Polarization transfer and the ratio $\mu_p G_E^p / G_M^p$: early Hall A results

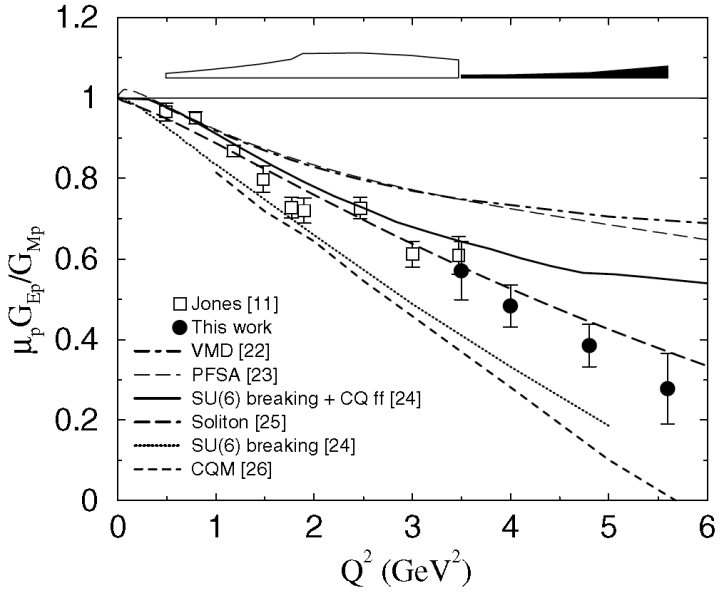

FIG. 2. The ratio $\mu_p G_{E_p}/G_{M_p}$ from this experiment and Jones *et al.* (Ref. [11]), compared with theoretical calculations. Systematic errors for both experiments are shown as a band at the top of the figure.

Gayou *et al.*, PRL 88, 092301 (2002) ("GEp-II")

- Figures at right are from Punjabi *et al.*, PRC 71, 055202 (2005)

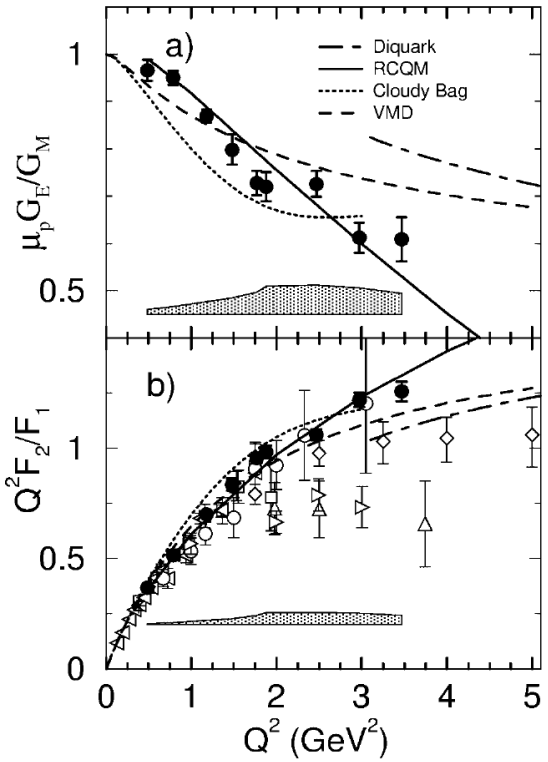

FIG. 2. (a) The ratio $\mu_p G_{E_p}/G_{M_p}$ from this experiment, compared with theoretical calculations. (b) The ratio $Q^2 F_{2_p}/F_{1_p}$ for the same data, compared to the same theoretical models as in (a) and world data; symbols as in Fig. 1. In both (a) and (b) the absolute value of systematic error from this experiment is shown by the shaded area.

Jones *et al.*, PRL 84, 1398 (2000) ("GEp-I")

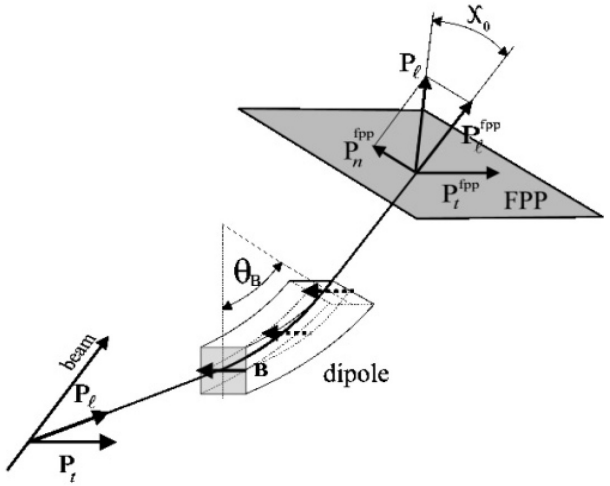

FIG. 15. Precession of the polarization component P_ℓ in the dipole of the HRS by an angle χ_θ.

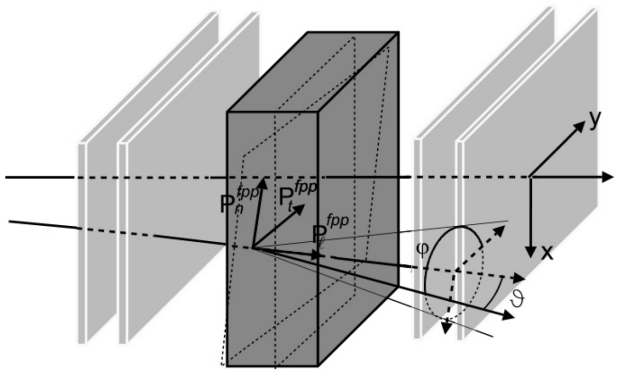

FIG. 9. Principle of the polarimeter, showing a noncentral trajectory through the front chambers, scattering in the analyzer, and a track through the back chambers; ϑ is the polar angle, and φ is the azimuthal angle from the y direction counterclockwise.

JLab Hall C 2007-2008: GEp-III and GEp-2γ

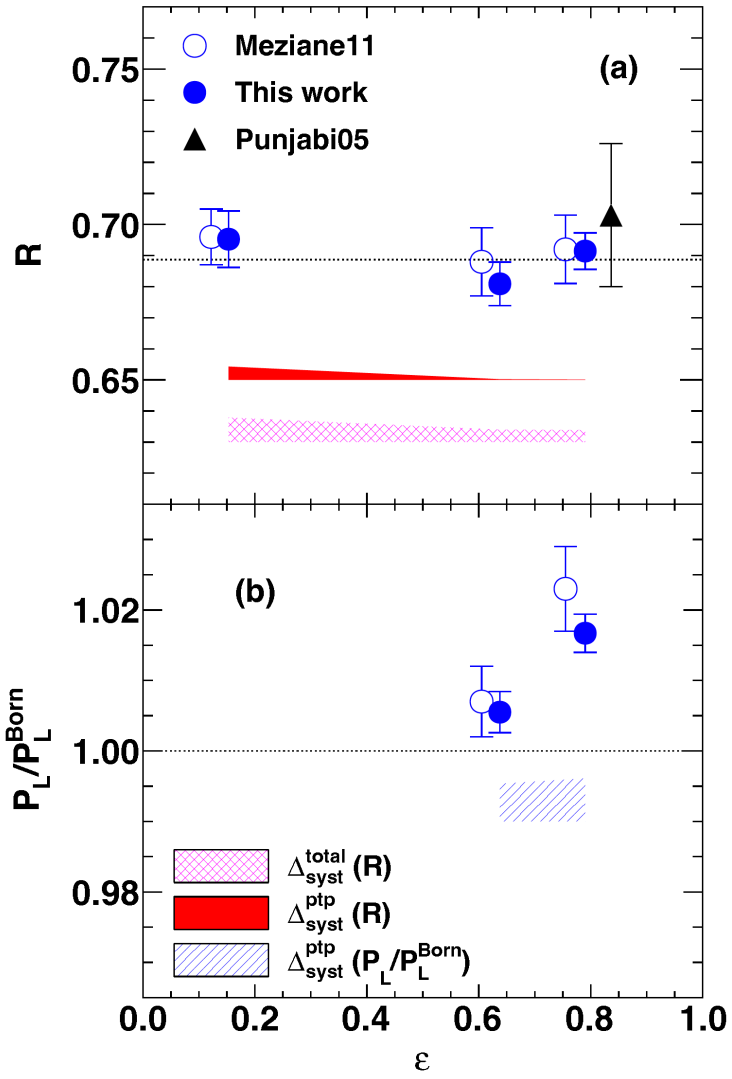

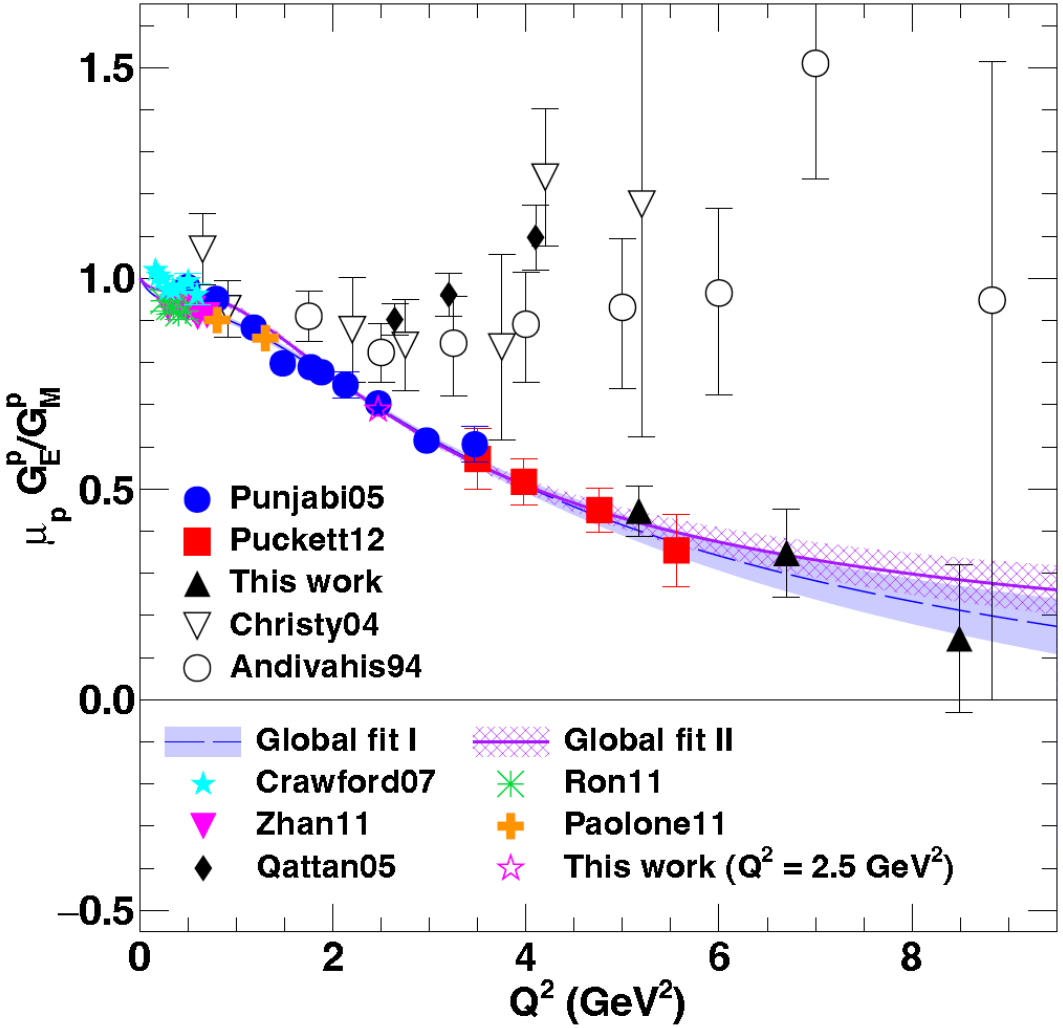

Puckett *et al.*, PRC 96, 055203 (2017)

Original publications

- Puckett *et al.*, PRL 104, 242301 (2010)
- Meziane *et al.*, PRL 106, 132501 (2011)
- See also GEp-I/II reanalyses/archival papers:
  - GEp-I: Punjabi *et al.*, PRC 71, 055202 (2005)
  - GEp-II: Puckett *et al.*, PRC 85, 045203 (2012)

Vanishing sensitivity of σ_R to high-Q^2 G_E^p

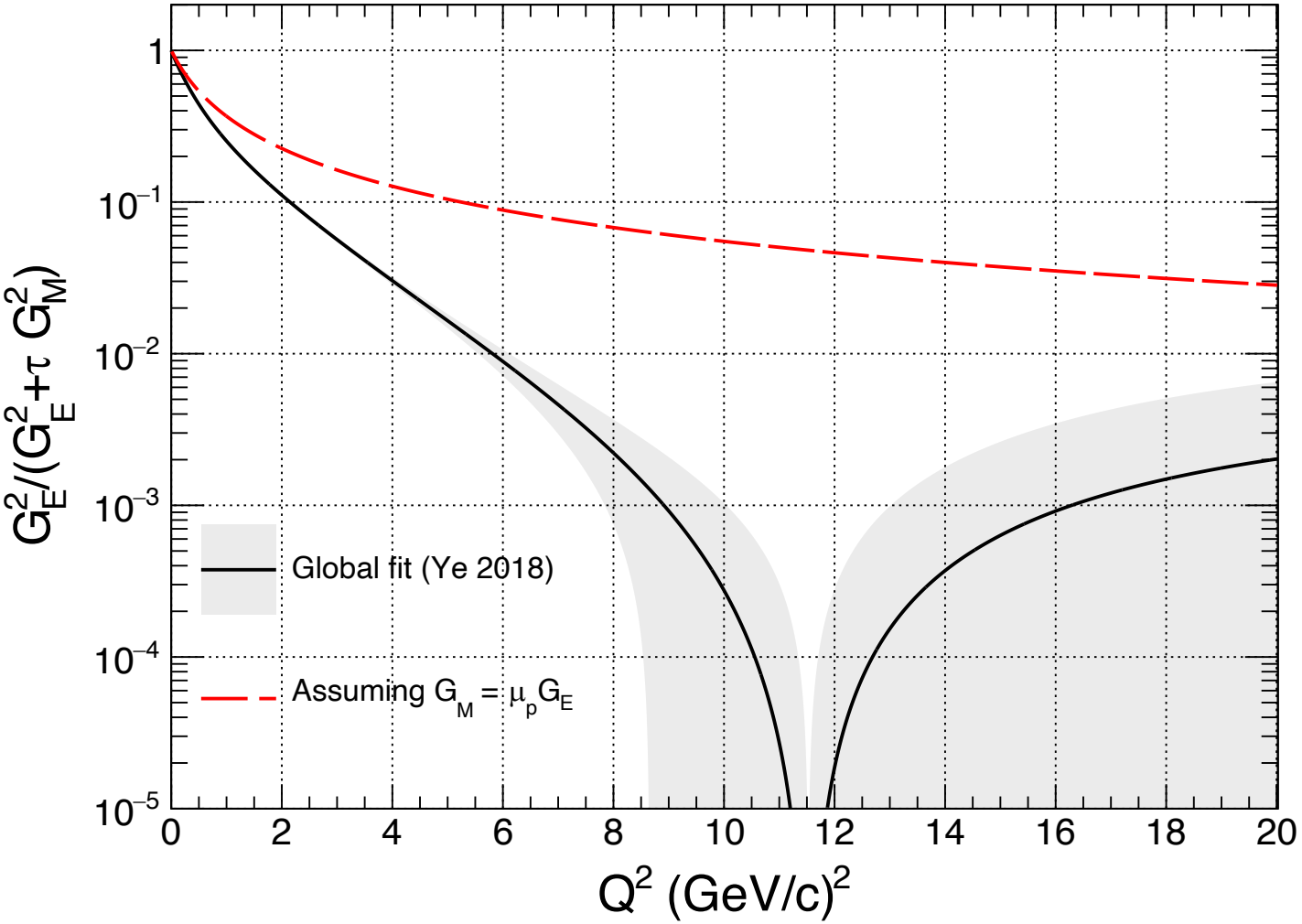

Given what we NOW know about the rapid fall-off of G_E^p above 1 GeV^2 (assuming polarization data give the "true" value) it is clear that the fractional electric contribution to the OPE cross section falls to a level at or below the limits of experimental and theoretical accuracy for Q^2 above a few GeV^2!

The APS Bonner Prize in Nuclear Physics, 2017

APS physics

2017 Tom W. Bonner Prize in Nuclear Physics Recipient

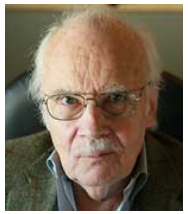

Charles F. Perdrisat
College of William and Mary

Citation:

"*For groundbreaking measurements of nucleon structure, and discovering the unexpected behavior of the magnetic and electric nucleon form factors with changing momentum transfer.*"

Background:

Charles F. Perdrisat, Ph.D., was a professor at the College of William and Mary (Williamsburg, Va.) for the last 50 years having retired earlier this year. Throughout his career, Dr. Perdrisat's research focus included nuclear reactions with proton and deuteron beams, both polarized and unpolarized. He conducted research at SATURNE in Saclay, France, TRIUMF in Vancouver, B.C., LAMPF in Los Alamos, New Mexico, Brookhaven National Laboratory in Upton, N.Y., and JINR in Dubna, Russia. During the last half of his career, he was committed to the investigation of the structure of the proton at Jefferson Laboratory, concentrating in obtaining polarization transfer data in the scattering of polarized electrons on unpolarized protons. These data, from 3 distinct experiments organized in close collaboration with Vina Punjabi, Ph.D., Mark K. Jones, Ph.D., Edward J. Brash, Ph.D., and Lubomir Pentchev, Ph.D., have resulted in a significant change of paradigm in the understanding of the structure of the nucleon. After completing his undergraduate training in physics and mathematics at the University of Geneva in 1956, Dr. Perdrisat became an assistant in the physics department at the Swiss Federal Institute of Technology in Zurich) in Switzerland, under Prof. Paul Scherrer; he received his Ph.D. in 1962. He completed a three-year postdoctoral fellowship at the University of Illinois Urbana-Champaign, before heading to William and Mary in 1966.

Selection Committee:

2017 Selection Committee Members: Rocco Schiavilla (Chair), D. Hertzog, P. Jacobs, Kate Jones, I-Y. Lee

Low-Q^2 $ep \to ep$ cross section data and proton radii

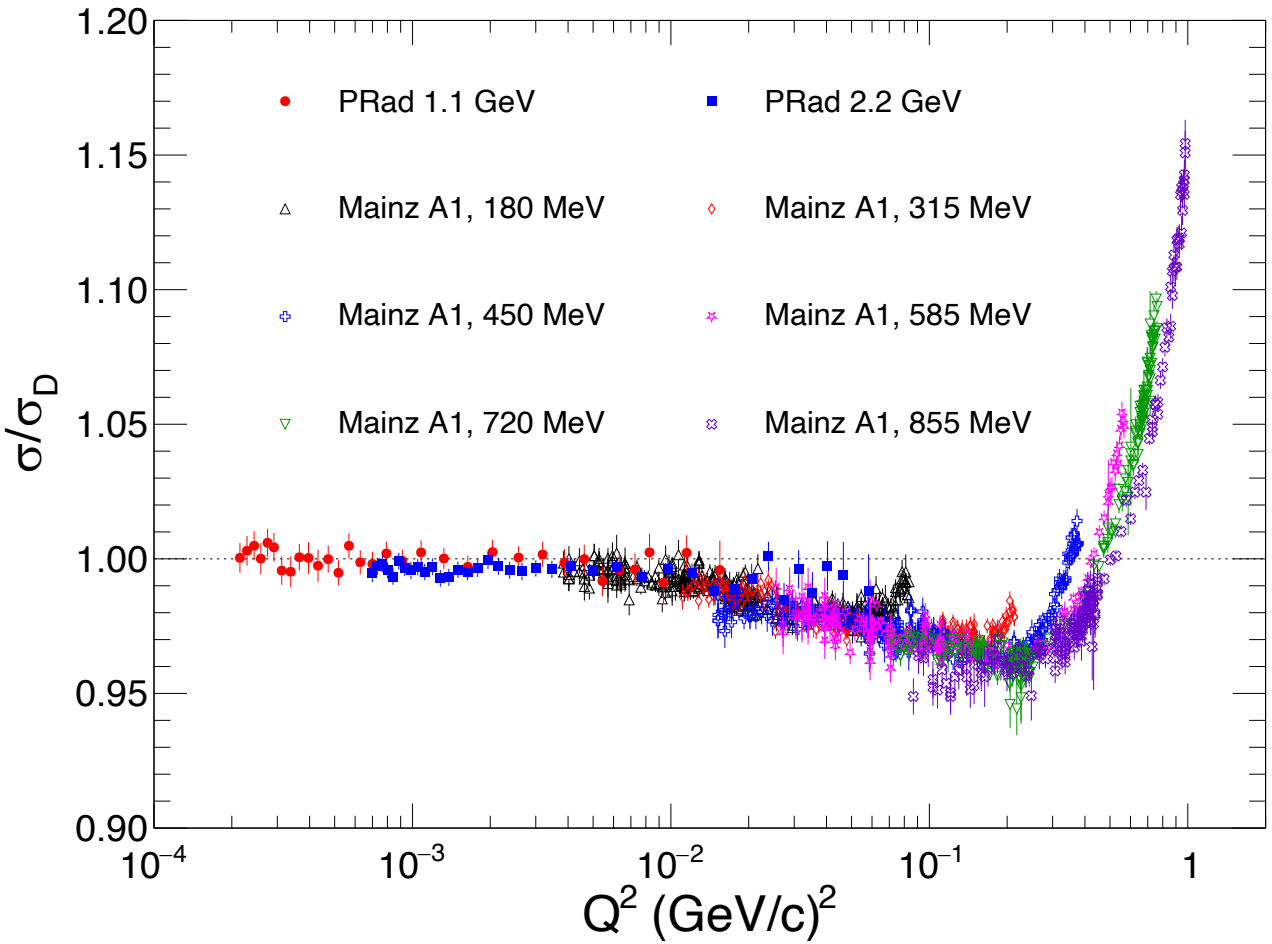

PRad and Mainz cross section data plotted as σ/σ_D, where $\sigma_D \equiv \sigma_{Mott} G_D^2 \left(\epsilon + \mu_p^2 \tau\right)/\left(\epsilon(1+\tau)\right)$

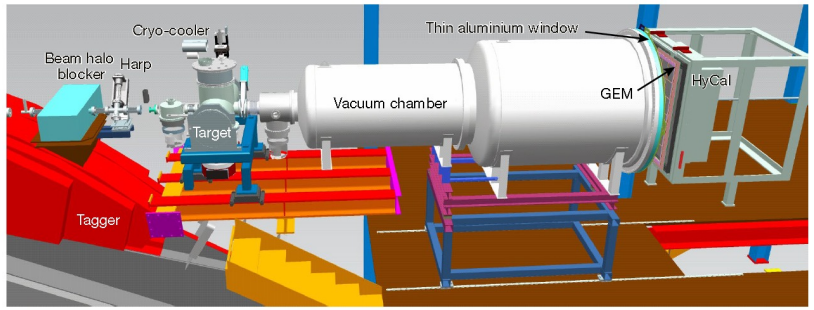

Fig. 1 | The PRad experimental setup. A schematic layout of the PRad experimental setup in Hall B at Jefferson Laboratory, with the electron beam incident from the left. The key beam-line elements are shown along with the windowless hydrogen gas target, the two-segment vacuum chamber and the two detector systems (see the Methods for a brief overview and the Supplementary Information for a description of the target and individual detectors).

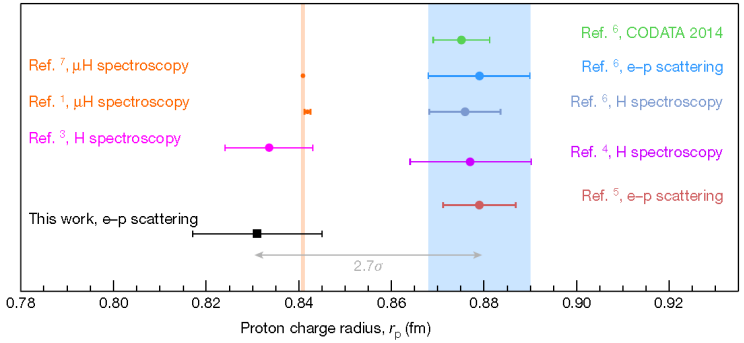

Fig. 4 | The proton charge radius. r_p as extracted from the PRad data in this work, shown alongside other measurements of r_p since 2010 and previous CODATA recommended values. Our result is 2.7σ smaller than the CODATA recommended value for e–p experiments[6]. The orange and blue vertical bands show the uncertainty bounds of the μH and CODATA values for e–p scattering, respectively.

- PRad results (Xiong *et al.,* Nature 575, 147 (2019)) consistent with muonic hydrogen results, whereas Mainz A1 results (Bernauer *et al.,* PRL 105, 242001 (2010) and PRC 90, 015206 (2014)) agree with older extractions based on electron scattering and ordinary hydrogen spectroscopy.
- Mainz G_M^p (and resulting magnetic radius) in significant tension with other world data.
- Mainz G_E^p/G_M^p, however, is consistent with recent (2011) precision low-Q^2 polarization data (see next slide)

Low-Q^2 $ep \to ep$ polarization data

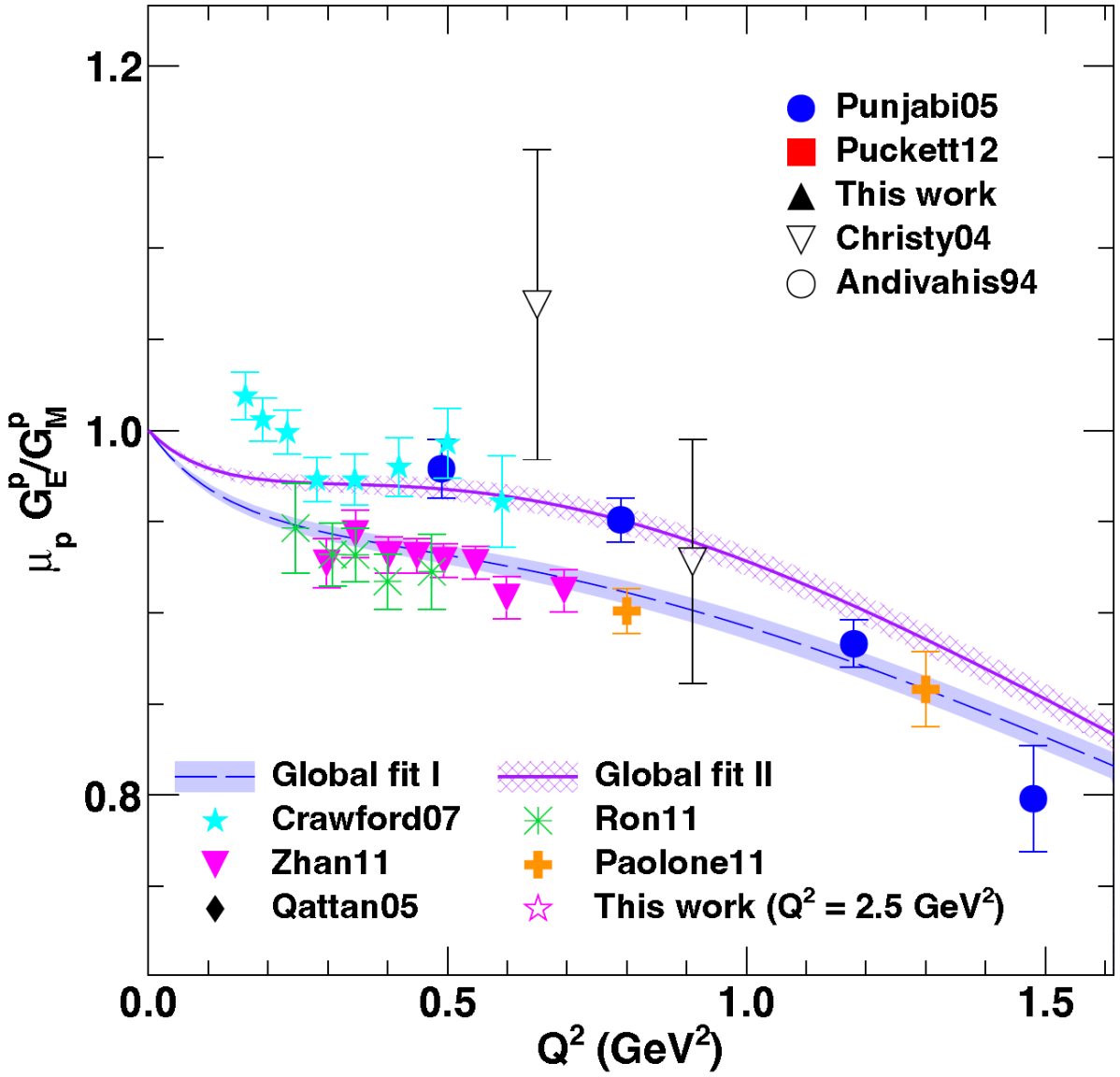

- While polarization observables are generally regarded as being the most reliable for the determination of G_E^p/G_M^p at large Q^2, a significant unresolved tension in the 0.1-1 GeV² region has existed since the 2010/2011 JLab Hall A publications by Ron, Zhan, and Paolone:
  - M. Paolone *et al.,* Phys. Rev. Lett. 105, 072001 (2010).
  - X. Zhan *et al.,* Phys. Lett. B 705, 59 (2011).
  - G. Ron *et al.,* PRC 84, 055204 (2011)
- A significant unknown systematic presumably exists in one or more of these data sets… would be nice for someone to dig into/reanalyze
- As noted on previous slide, the more recent polarization data favor a lower G_E/G_M ratio, consistent with Mainz A1 data, which favor a higher G_M value at low Q^2 compared to other world data
- Low-Q^2 polarized-target G_E^p data were collected by Hall A ~2012… still under analysis.
- Issues accumulating with internal consistency of elastic $ep \to ep$ data at low Q^2 as we keep pushing the precision envelope…

The discrepancy at large Q^2 and hard TPE

A. Afanasev et al. / Progress in Particle and Nuclear Physics 95 (2017) 245–278

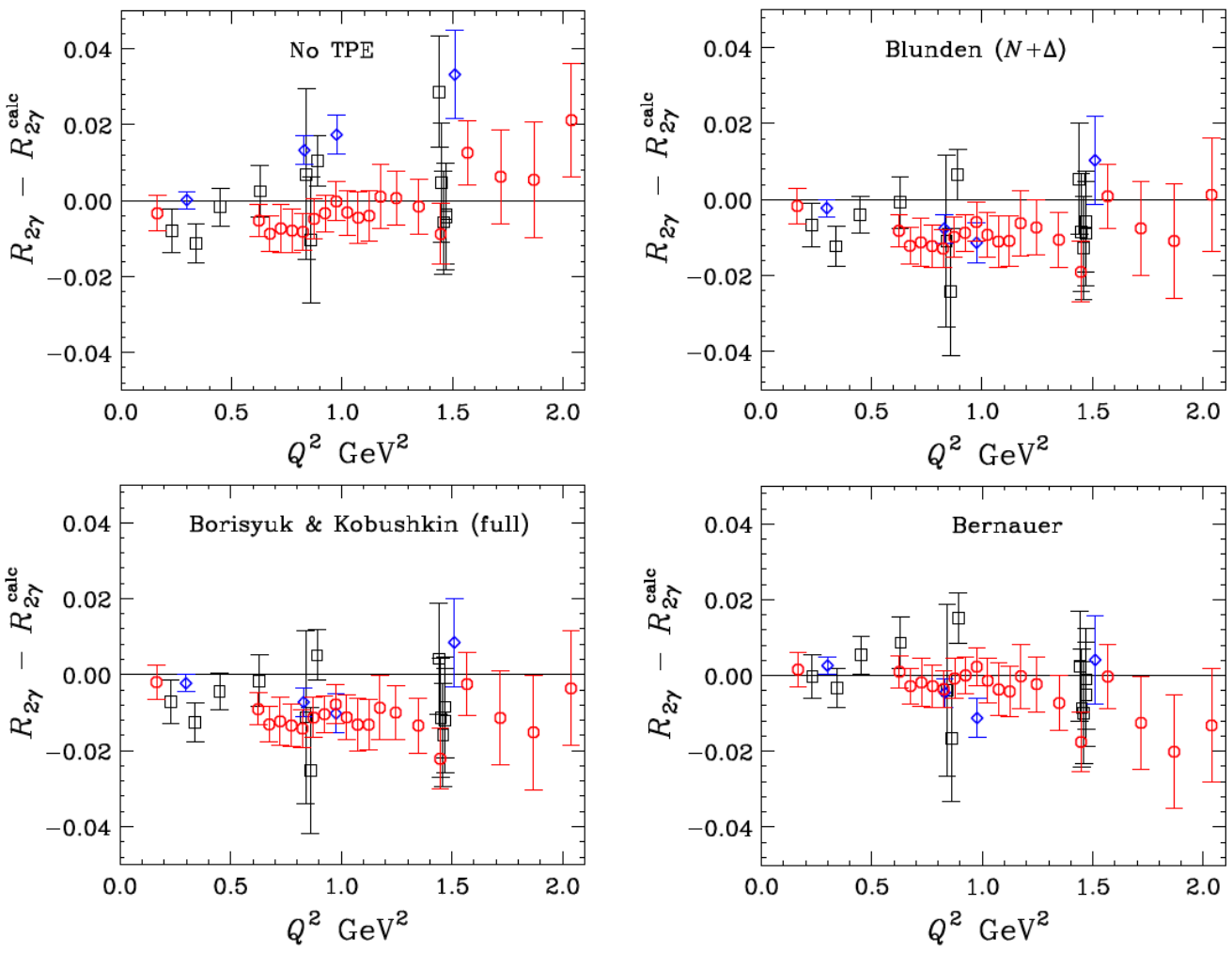

Fig. 3.16. Difference between $R_{2\gamma}$ and model predictions as a function of Q^2. Data symbols are the same as in Fig. 3.15.

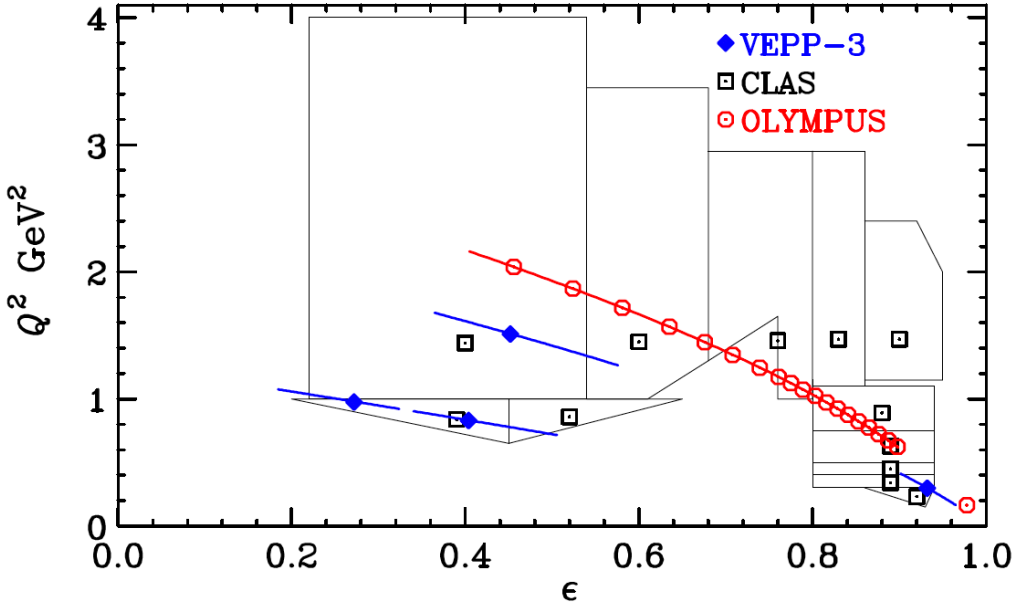

- Three dedicated experiments looked at e^+p/e^-p cross section ratio as a direct measurement of the TPE contribution to the scattering.
- Did not reach high enough Q^2 and/or low-enough ϵ to conclusively answer whether hard TPE resolves the discrepancy.
- Major motivation for developing a positron source at CEBAF

New precision high-Q cross sections and TPE

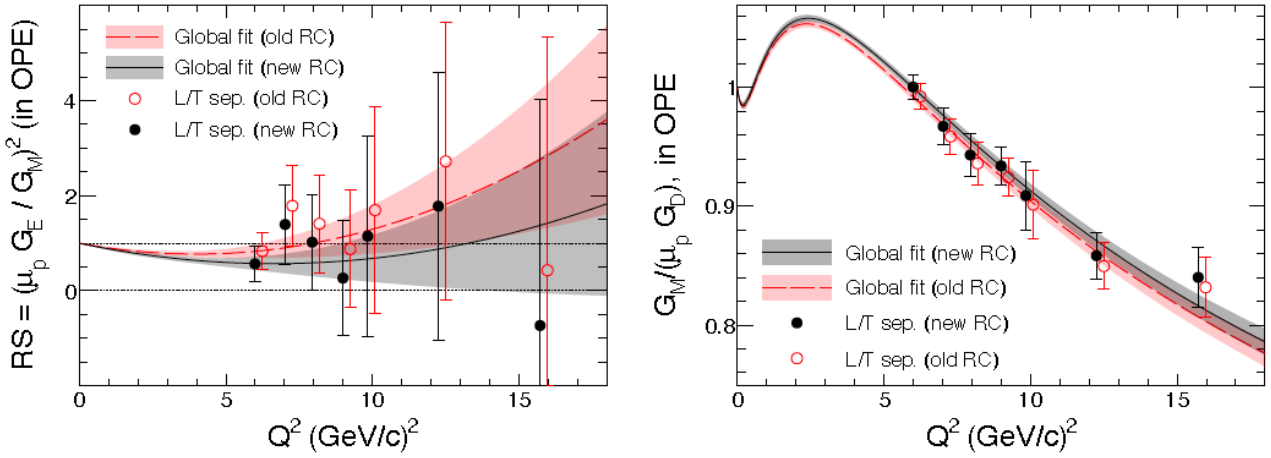

FIG. 5. Impact of applying the radiative corrections of Ref. [1] on the Rosenbluth slope (left) and $G_M/(\mu_p G_D)$ (right). In both panels, the black solid (red dashed) curve shows the global fit result using the cross sections with modified (originally published) radiative corrections. The black filled circles (red empty circles) show the L/T separation results obtained using the modified (originally published) radiative corrections. In both plots, the results obtained using the originally published radiative corrections have been offset by +0.25 $(\mathrm{GeV}/c)^2$ in Q^2 for clarity.

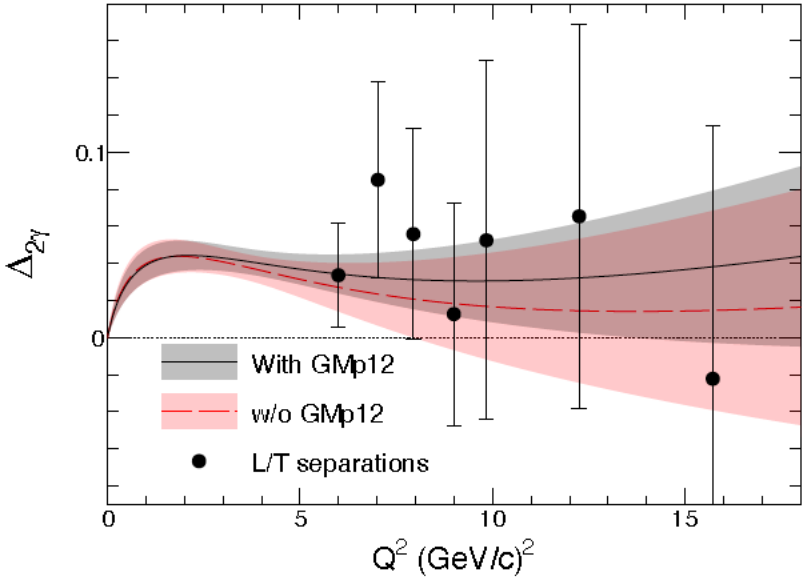

- From supplemental material to Christy *et al.*, PRL 128, 102002 (2022) https://journals.aps.org/prl/supplemental/10.1103/PhysRevLett.128.102002
- See Bogdan's talk (next) for more details.
- New L/T separations in the 6-16 GeV^2 region.
- Updated radiative corrections for JLab and SLAC high-Q data
- TPE contribution of ~4% required to account for the discrepancy in Rosenbluth Slope
- Impact of updating RCs for older experiments to more accurate Maximon-Tjon prescription is to reduce the significance of the discrepancy in the high-Q region from ~3σ to ~2σ.

Springer Link

Search Log in

Editorial | Published: 14 March 2022

Topical issue on an experimental program with positron beams at Jefferson Lab

Nicolas Alamanos, Marco Battaglieri, Douglas Higinbotham, Silvia Niccolai, Axel Schmidt & Eric Voutier

The European Physical Journal A **58**, Article number: 45 (2022) | Cite this article

The interest in high energy and high duty cycle polarized and unpolarized positron beams, in complement to the existing CEBAF (Continuous Electron Beam Accelerator Facility) electron beams, has been nurtured since the very first energy upgrade of the accelerator up to 6 GeV. Along the years, experimental results about the electromagnetic form factors and the generalized parton distributions of the nucleon pointed towards the importance of positron

Download PDF

Part of a collection:

An Experimental Program with Positron Beams at Jefferson Lab

Sections References

https://link.springer.com/article/10.1140/epja/s10050-022-00699-6

G_E^p World Data Summary

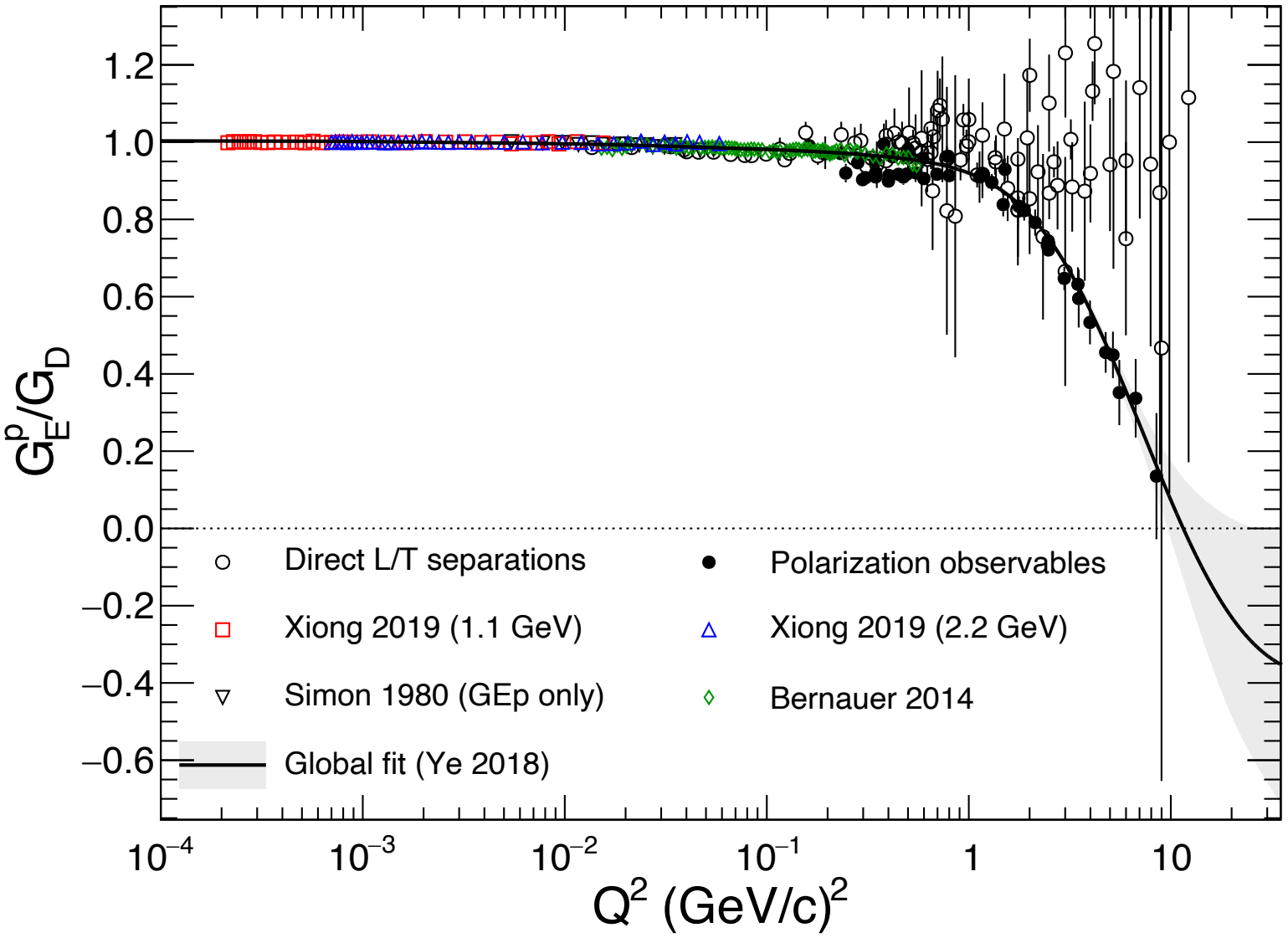

- "Direct L/T separations" = published point extractions of G_E^2, G_M^2 from Rosenbluth plots (not all points totally independent)
- "Polarization observables" = polarized beam-target asymmetry and recoil polarization data
- "Bernauer 2014" = direct Rosenbluth separations from Mainz A1, Bernauer *et al.*, PRC 90, 015206 (2014)
- "Xiong 2019" = PRad experiment, W. Xiong *et al.,* Nature 575, 147 (2019)
- Global fit curve is from Ye *et al.,* Phys. Lett. B 777, 8 (2018)

G_M^p World Data Summary

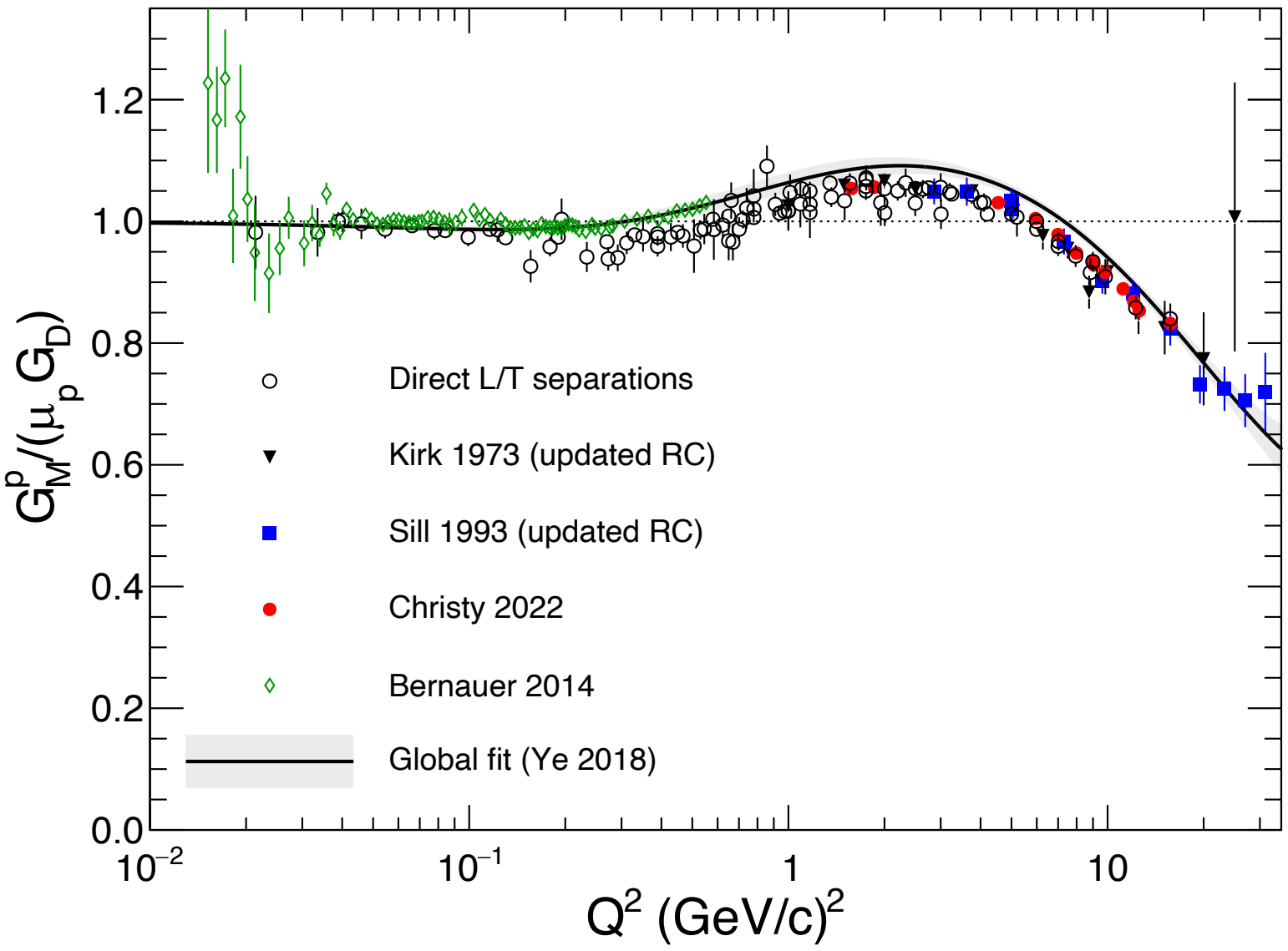

- "Direct L/T separations" = published point extractions of G_E^2, G_M^2 from Rosenbluth plots (not all points totally independent)
- Kirk 1973, Sill 1993, and Christy 2022 are point G_M^p extractions from individual cross section measurements, with "state-of-the-art" radiative corrections as described in Christy *et al.,* PRL 128, 102002 (2022)
- "Bernauer 2014" = direct Rosenbluth separations from Mainz A1, Bernauer *et al.*, PRC 90, 015206 (2014)
- Global fit curve is from Ye *et al.,* Phys. Lett. B 777, 8 (2018) (NOTE: includes Hard TPE corrections absent from most published extractions)

Summary of Proton Data

- **Including the recent PRAD data, elastic $ep \rightarrow ep$ scattering has been measured over ~5 orders of magnitude in Q^2, and roughly 16! orders of magnitude in $d\sigma/d\Omega_e$**
- High-Q discrepancy between cross sections and polarization observables has exposed the limits of applicability of the one-photon-exchange approximation, and completely changed our basic notions of proton size, shape, and structure (importance of quark orbital angular momentum, diquark correlations, relativistic effects in quark wavefunctions, etc)
- Significant issues have also emerged at low-Q^2, as the envelope of experimental precision has been pushed
- Advancing physical intuition/insight and guiding improvement of theoretical calculations also requires improving the *neutron* data and extending the high-Q reach of the proton data, as well as developing a unified interpretation of FFs in the spacelike and timelike regions (See E. T-G. talk later in this session!)

Neutron Form Factors

- More difficult to measure than the proton due to lack of free neutron targets
- Far less accurately known than the proton FFs over a far more limited Q^2 range
- Cross section dominated by G_M^n over most of measured Q^2 range
- Most reliable G_E^n data come from polarization observables
- Most reliable G_M^n data come from "ratio" method on deuterium: first proposed by Durand, Phys. Rev. 115, 1020 (1959)
  - Some extractions also exist from absolute cross section and polarization measurements

"Ratio" method for G_M^n

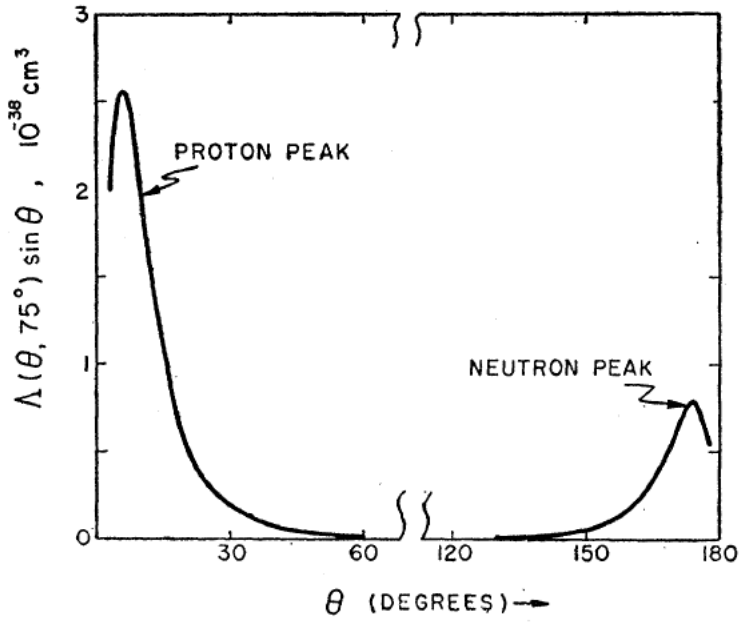

FIG. 1. The angular distribution function $\Lambda(\theta,\vartheta)\sin\theta$ in the absence of final-state interactions is plotted as a function of the proton scattering angle in the nucleon center-of-mass system $[\cos\theta=\hat{p}\cdot\hat{q}]$ for the scattering of 500-Mev electrons through an angle $\vartheta=75°$ with a momentum transfer giving $p=\frac{1}{2}q=1.3\times10^{13}$ cm^{-1}. $\Lambda(\theta,\vartheta)$ is defined in Eq. (11.2); the function $F(\theta)$ entering the definition was evaluated using a Hulthén wave function for the deuteron. The cross section $d^3\sigma/(d\theta d\Omega_e dE_e')$ is given by $(4.71\times10^5$ cm^{-1} rad^{-1} sterad^{-1} Mev$^{-1})$ $\Lambda(\theta,\vartheta)\sin\theta$. No nucleon form factors have been introduced into the results.

Figure from Durand, 1959 (see previous slide for reference)

- Idea: simultaneous measurement of $d(e,e'n)p$ and $d(e,e'p)n$ in quasi-elastic kinematics
- Simultaneous measurement cancels many sources of experimental systematic uncertainty (electron acceptance/detection efficiency, luminosity, detector and DAQ livetime, etc).
- Small nuclear model dependence—nuclear effects similar/nearly identical for (e,e'n) and (e,e'p) cross sections
- Combine with existing knowledge of free proton cross section to extract free neutron cross section
- **Major remaining source of systematic uncertainty is the relative acceptance/efficiency between protons and neutrons! → SBS-HCAL was designed to minimize this**

G_M^n World Data Summary

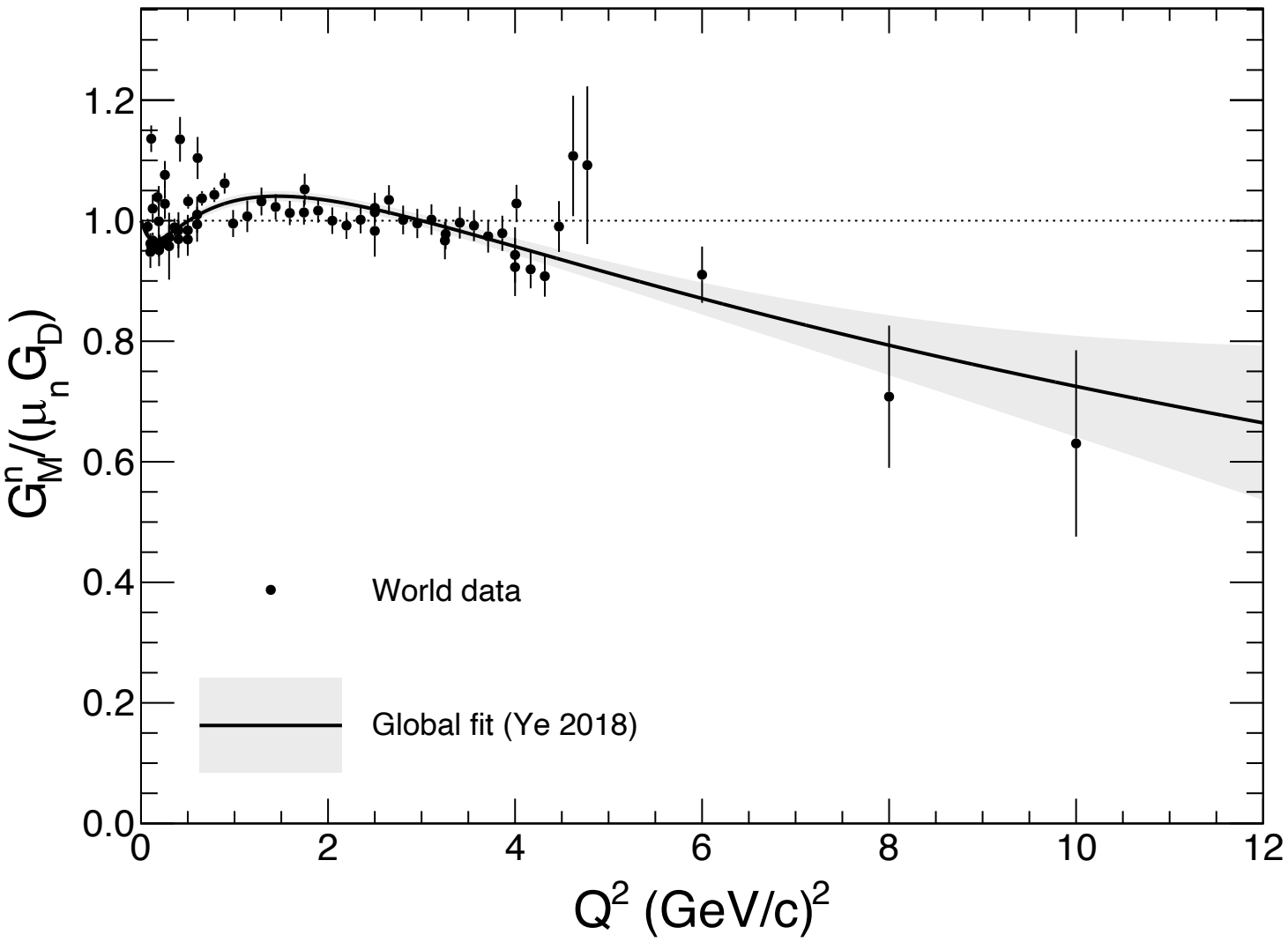

- Precise data only reach $Q^2 \approx 4.5$ GeV^2
- References for "world data" are the same as given in the caption to Figure 17 of Puckett *et al.*, PRC 85, 045203 (2012)
- Measurements out to 10 GeV^2 exist with very large uncertainties (Rock *et al.*, PRL 49, 1139 (1982) and PRD 46, 24 (1992)
- Most precise data with widest Q^2 coverage are from CLAS Collaboration: J. D. Lachniet *et al.*, PRL 102, 192001 (2009) from 1-4.8 GeV^2 using ratio method
- Other measurements used either inclusive quasi-elastic double-spin asymmetry on polarized Helium-3, or absolute cross section measurements on inclusive d(e,e') or coincidence d(e,e'n)

G_E^n data (plots from Obrecht *et al.*, in preparation)

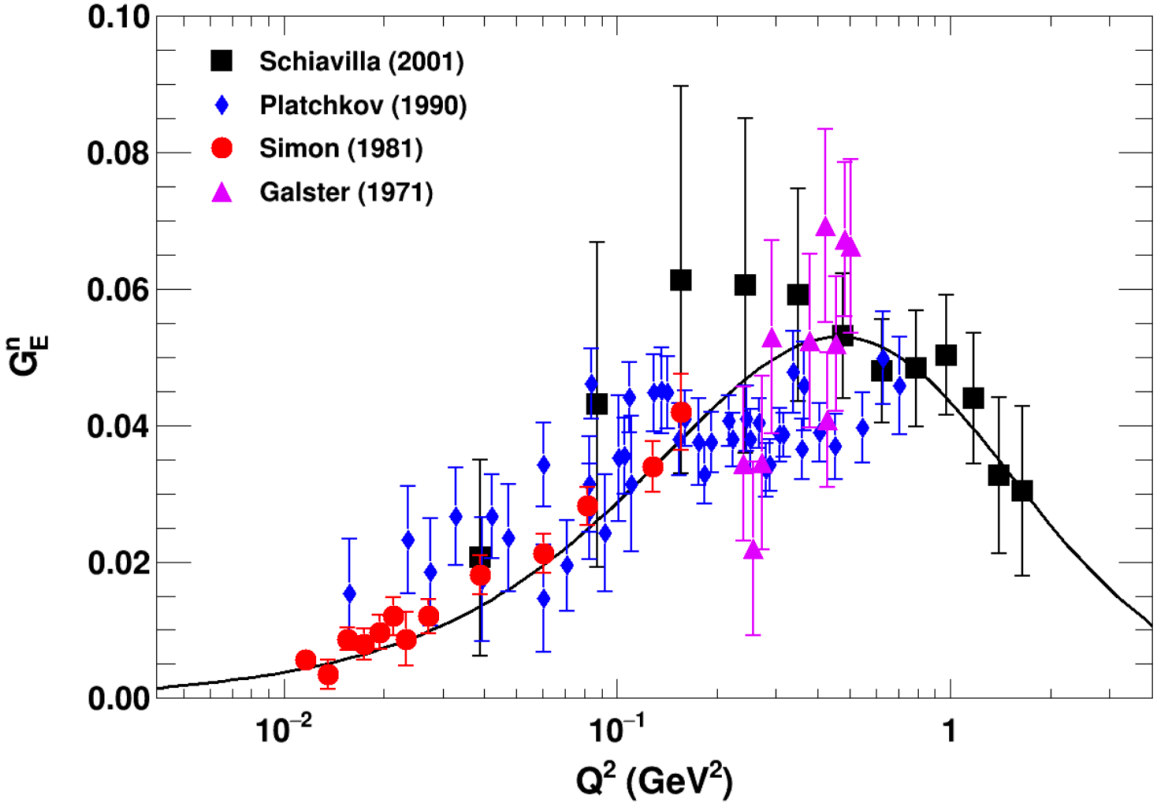

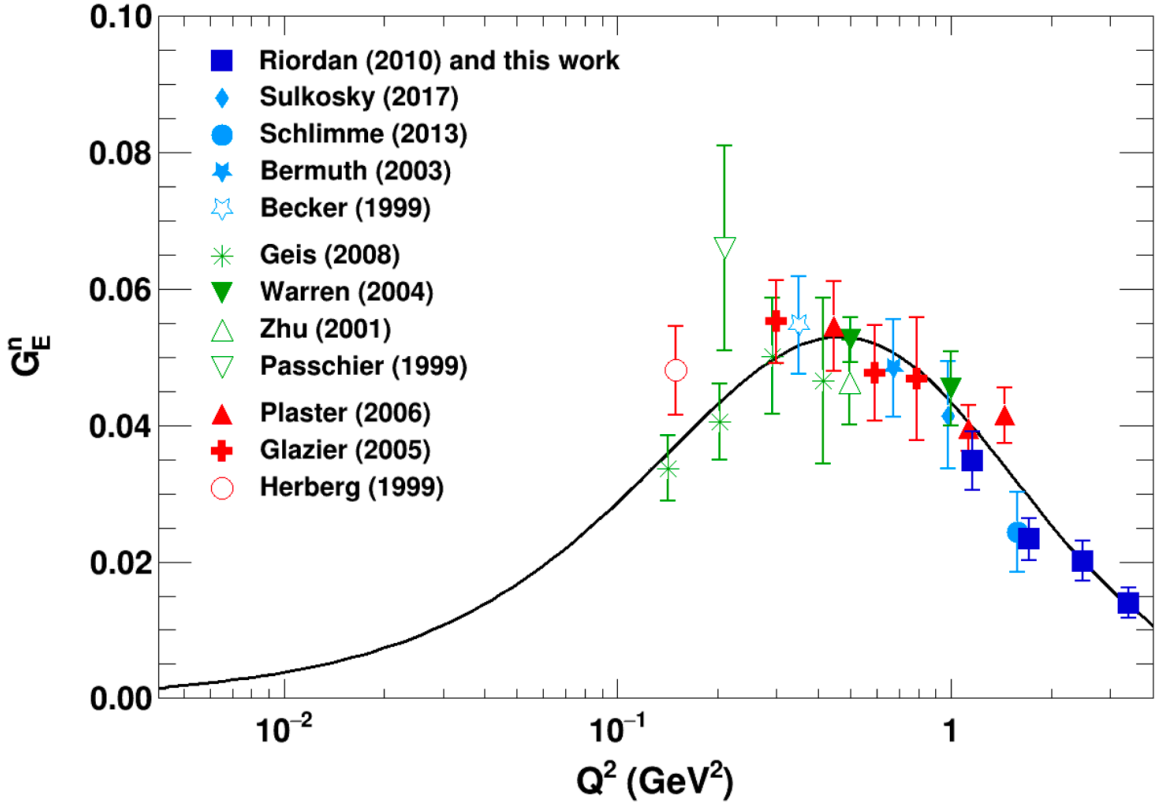

- Left: Older extractions of G_E^n from elastic *ed* cross section measurements… generally considered less reliable than polarization observables in quasi-elastic scattering, but qualitatively consistent, to within (large) uncertainties
- Right: extractions of G_E^n from polarization observables (color-coded by observable): Polarized Helium-3 target asymmetry, Deuteron recoil polarimetry, Polarized deuterium target asymmetry
- See Freddy Obrecht Ph.D. thesis: https://opencommons.uconn.edu/dissertations/2045/

G_E^n World Data Summary

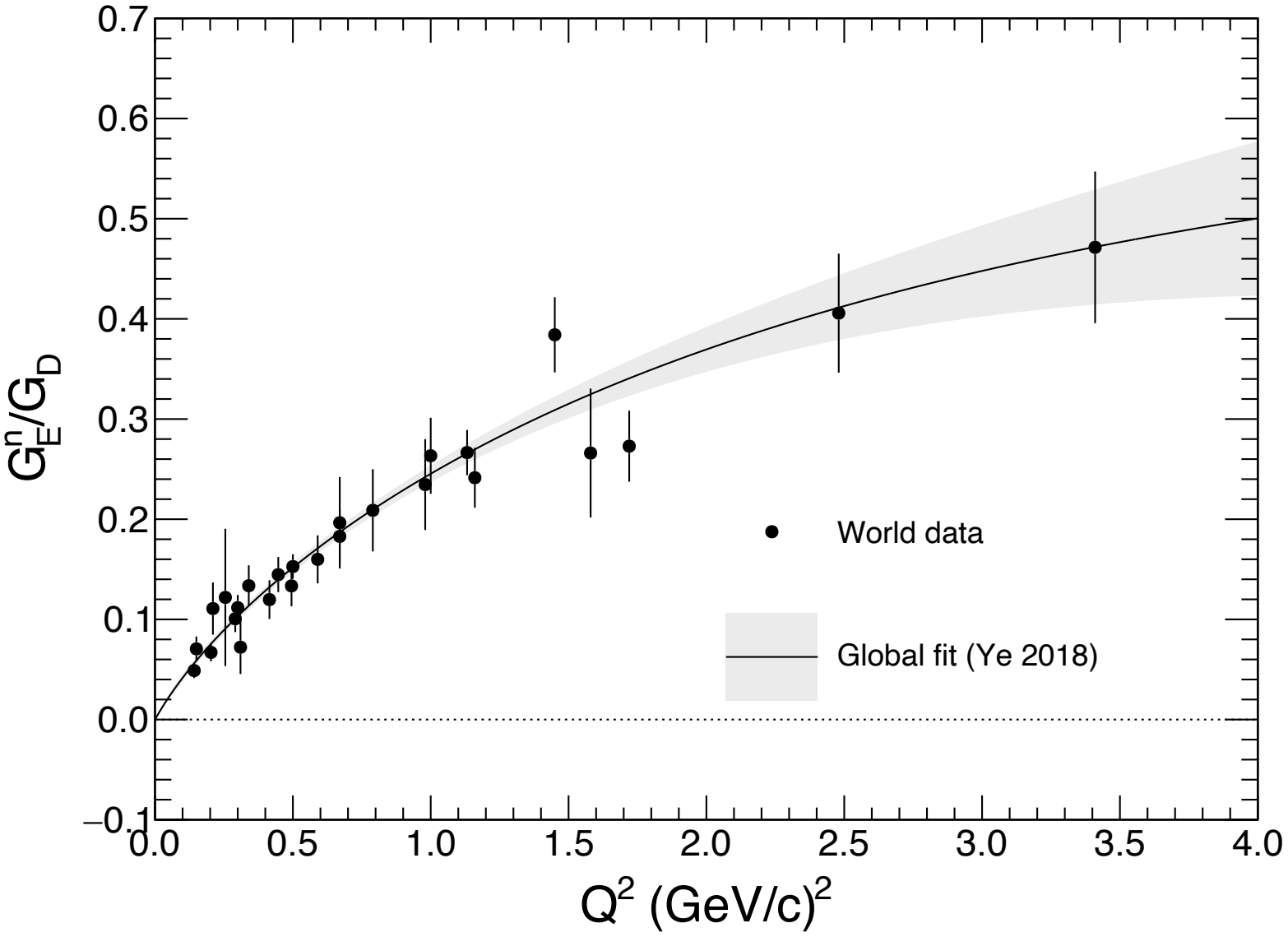

- G_E^n is the least well-known of the nucleon spacelike EMFFs
- New measurements up to ~10 GeV² planned in the near future by SBS Collaboration in Hall A at JLab (starting in about 3 weeks from today; see Bogdan W. talk after this one)
- Neutron FF data will complete the full flavor decomposition of F_1, F_2 over the Q^2 range accessible with JLab 12 GeV

SBS era has started in Hall A!

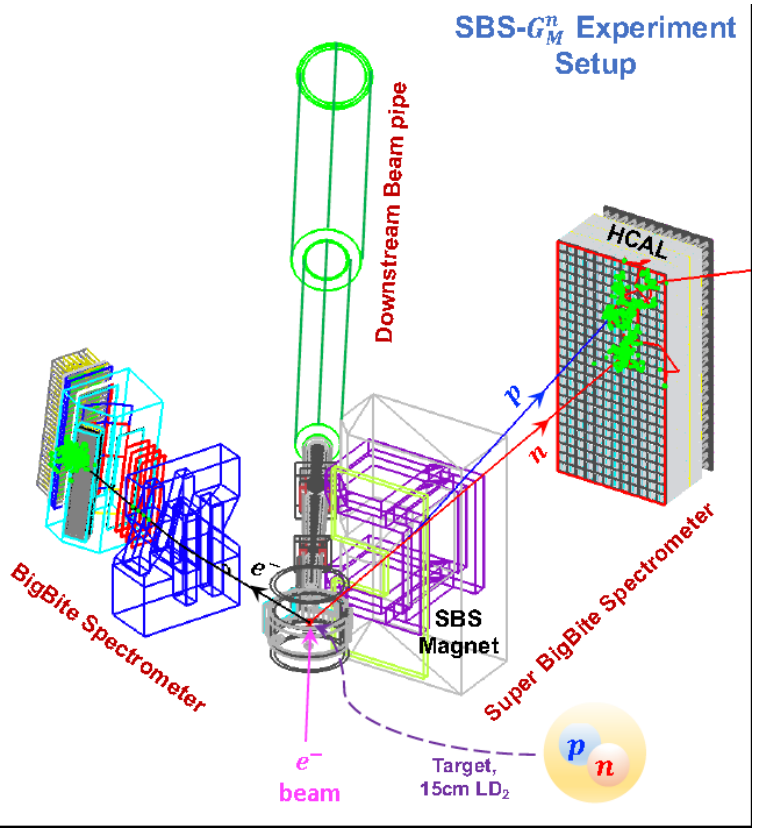

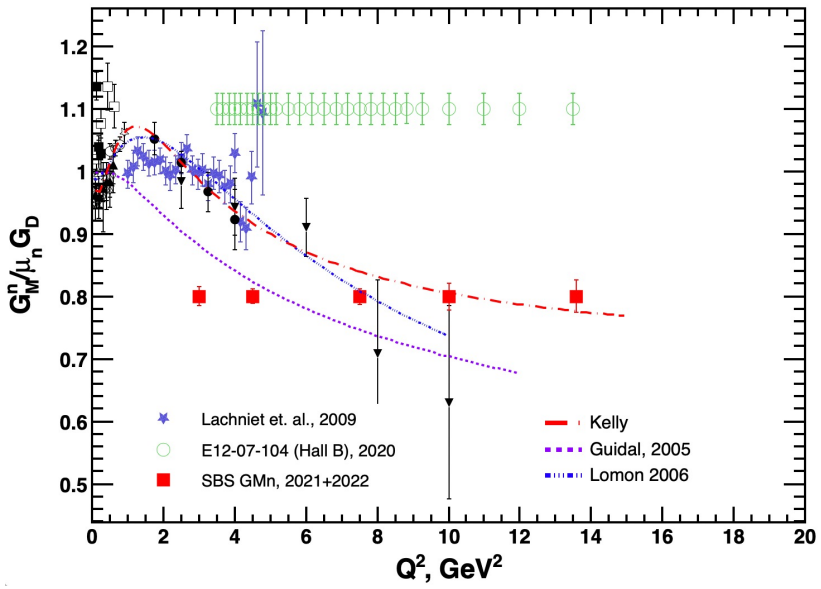

Above: Projected uncertainties and Q^2 points based on data collected

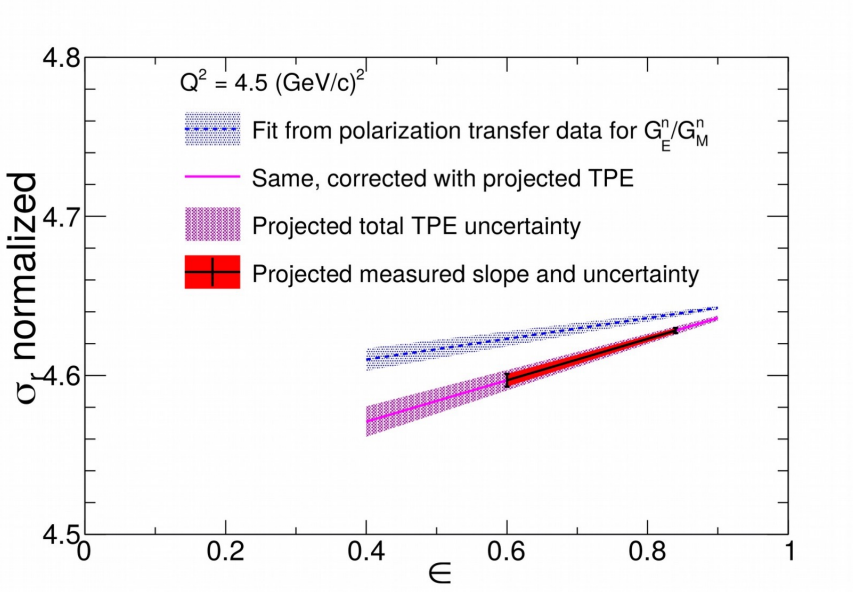

Neutron Rosenbluth Slope expected precision at 4.5 GeV^2

"GMN" family of experiments (E12-09-019 and E12-20-010) completed Oct. 2021-Feb. 2022,
Luminosities up to 10^{38} electron/s × nucleons/cm^2

Early SBS-GMN analysis highlights

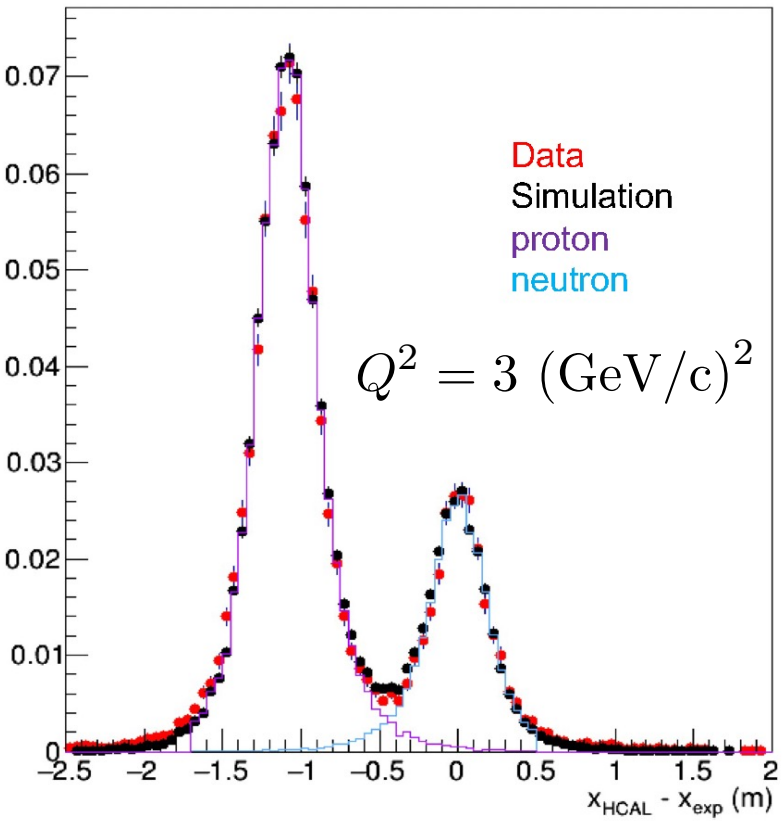

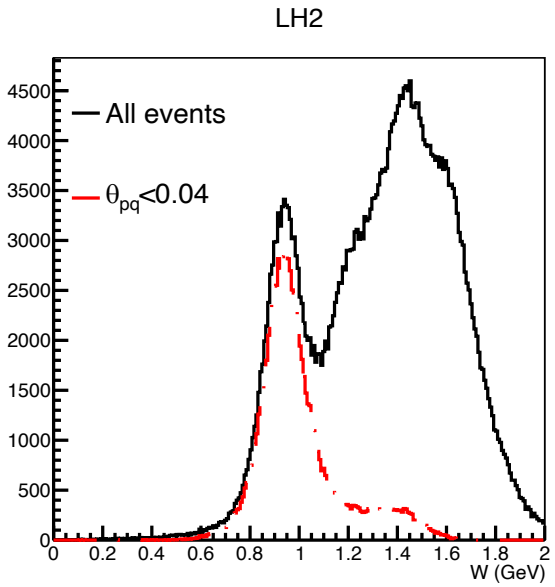

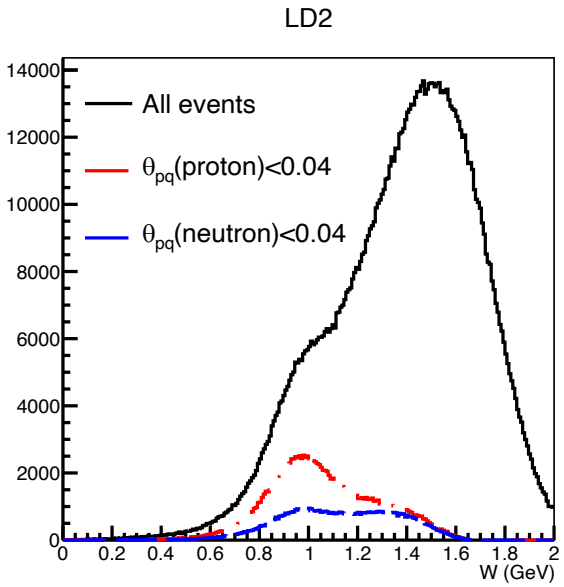

$$Q^2 = 4.5\ (\mathrm{GeV/c})^2$$
$$E_e = 6\ \mathrm{GeV}$$

- Real data-Monte Carlo comparison at $Q^2 = 3\ GeV^2$ (where SBS data overlaps Hall B)
- Figure from Provakar Datta (UConn)

- Above: Hydrogen (left) and deuterium (right) invariant mass distributions, with and without nucleon cuts
- Right: difference between predicted and measured vertical coordinate at HCAL
- Both plots for E = 6 GeV, Q^2 = 4.5

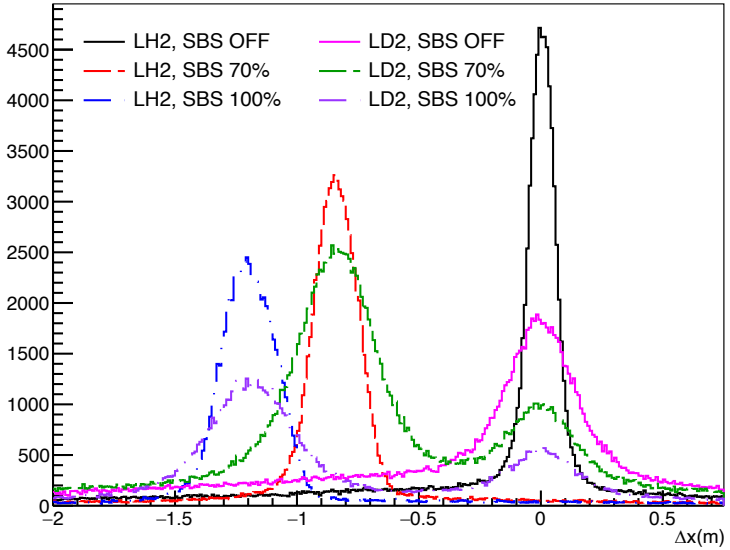

SBS GMn—Quasi-elastic event selection, LD2, $Q^2 = 10\ GeV^2$

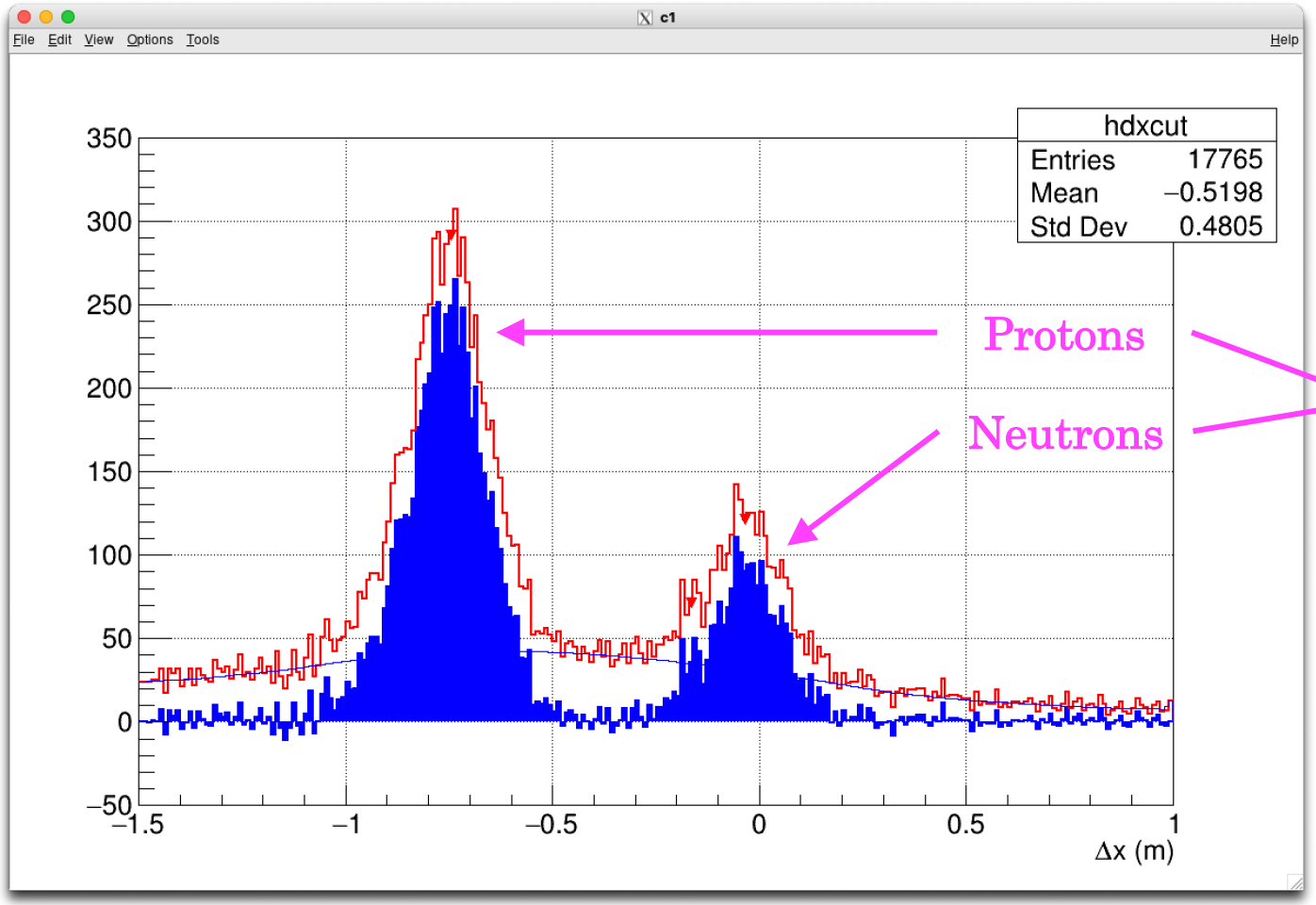

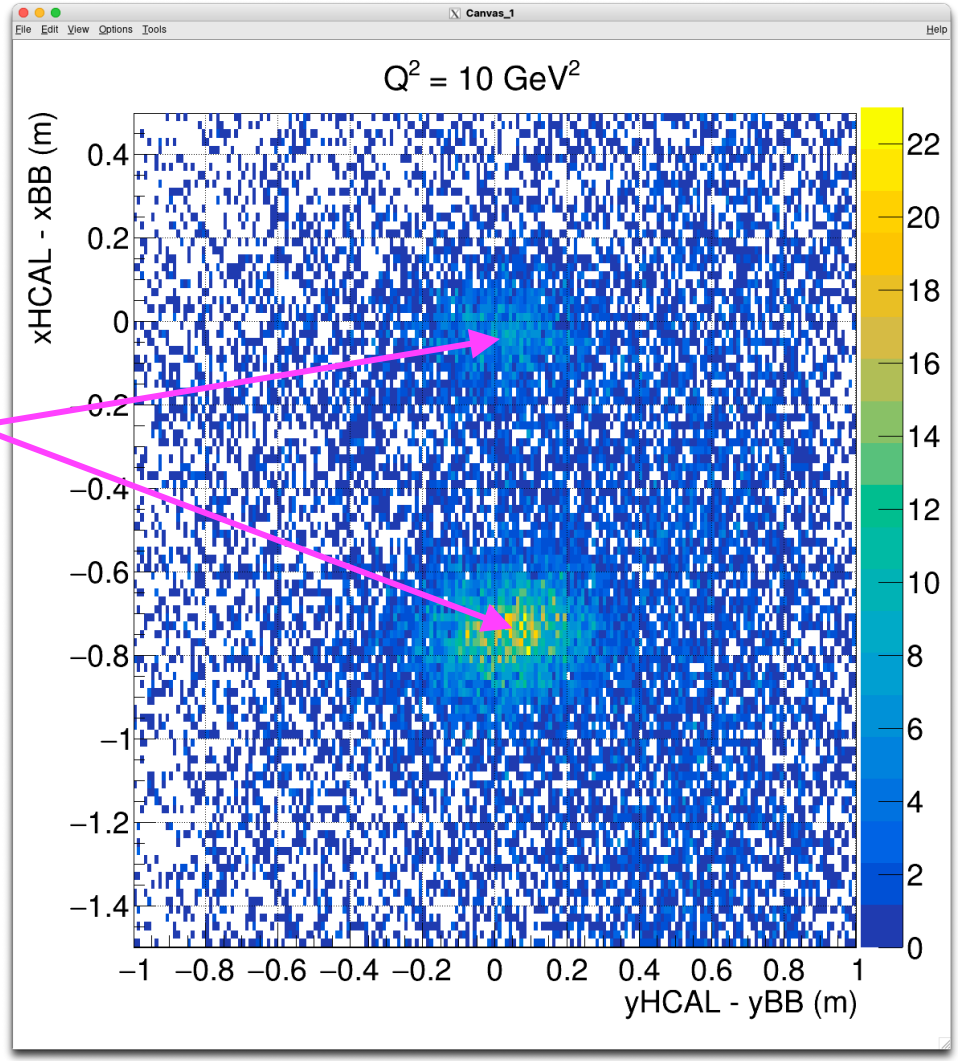

$$0 \leq W \leq 1.2\ \text{GeV}$$

Summary of Spacelike EMFFs with projected SBS results, selected theoretical models, global fit

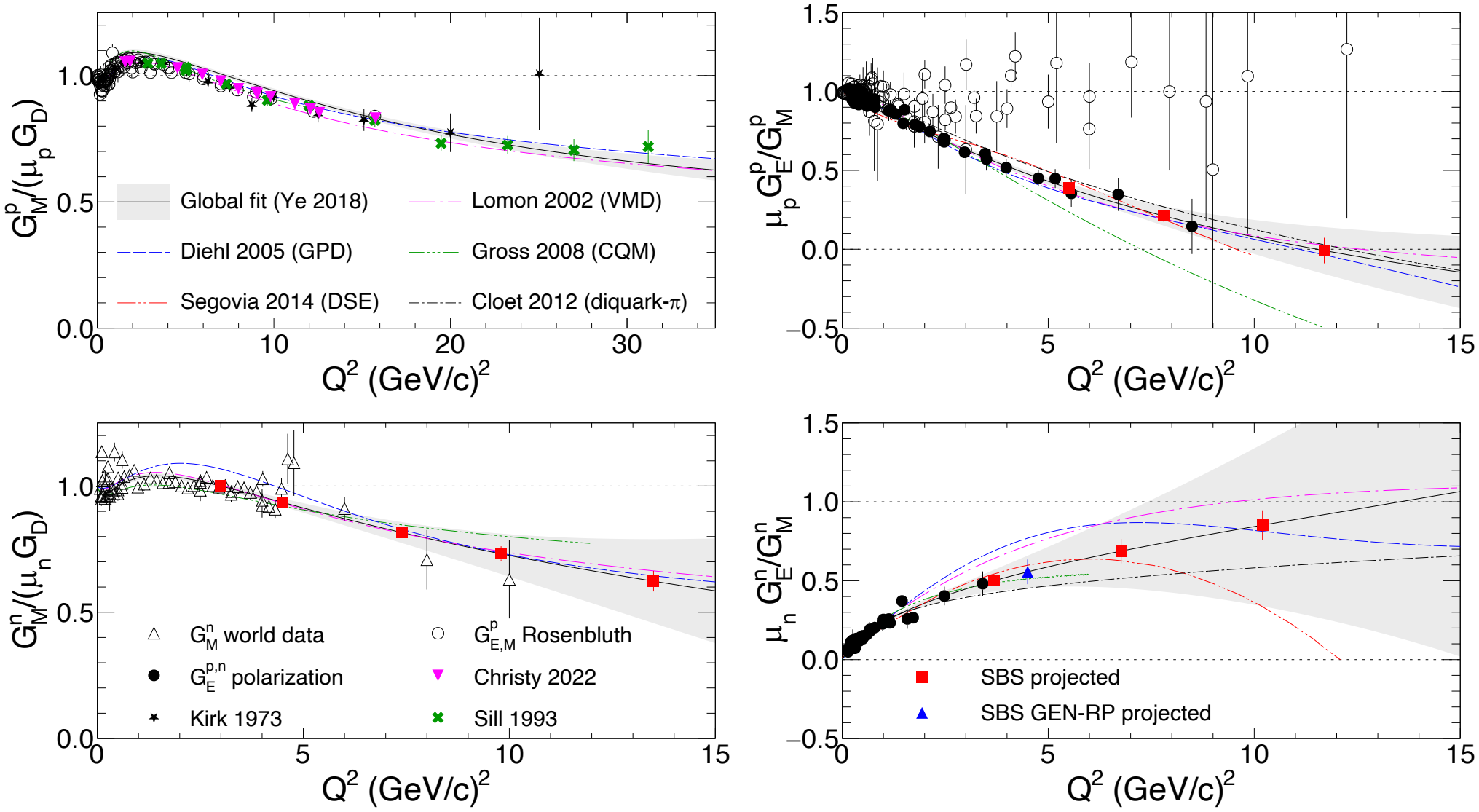

Summary and Conclusions

- Nucleon EMFF measurements have a rich history of discovery; as well-defined fundamental properties of the nucleon, they provide essential guidance and benchmarks to improve theoretical calculations of nucleon structure
- New data at high Q^2, ***despite the difficulty of the experiments***, always attract lots of theoretical attention; a large share of the most-cited papers from Jefferson Lab address the elastic form factors
- Good knowledge of FFs over entire practically accessible range of energies is needed as input for the interpretation of many other experiments in nuclear physics including GPDs, A(e,e'p), etc.
- The SBS high-Q^2 form factor program has started in Hall A and will be completed over the next several years:
  - GMN: Completed 2021-2022
  - GEN-Helium-3: Starting in ~3 weeks, run through March 2023
  - GEN-recoil polarization: expected running summer 2023
  - GEP recoil polarization: expected fall 2023-spring 2024
- After SBS, the potential exists to reach even higher Q^2 with EIC or the JLab "20 GeV" upgrade